Exploring para-thiophenols to expand the SAR of antimalarial 3-indolylethanones

A thesis submitted in fulfilment of the

requirements for the degree of

Master of Science (Pharmacy)

Of

Rhodes University

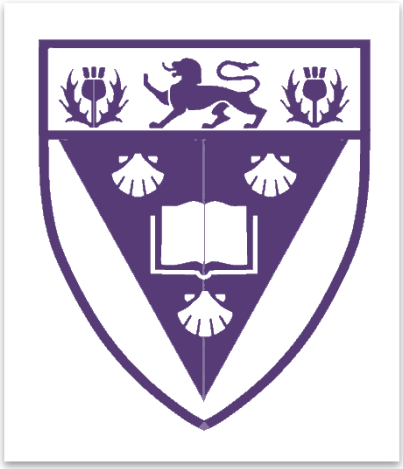

By

Ruramai Lissa Chisango

January 2018

Abstract

According to the WHO, malaria is responsible for over half a million deaths annually especially in populations from disadvantaged settings. Although there has been a documented improvement in the mortality rates, malaria has proved to be a global emergency. Mostly affecting the poor population, this disease is perpetuating a vicious cycle of poverty in the developing world as current preventive measures are not adequate unless adopted in addition to effective treatment. However, there has been a worldwide increase in resistance to available treatment which presents a need for novel, affordable treatment.

A study conducted in our laboratory identified two hit thiophenol containing compounds **2.24** and **2.25**. These molecules provided initial insight into the SAR and potential pharmacophore of this class of compounds. We decided to further explore these compounds by making bioisosteric replacements to optimize the structure as we monitor the effect of these modifications on the anti-plasmodial activity.

The synthetic pathway to form the target compounds of our study comprised of three steps which were initiated by the Friedel-Crafts acetylation of the indoles resulting in compounds **3.5** – **3.7**. A bromination step followed which yielded the α-bromo ketones (**3.8** – **3.11**). Some of the thiophenols (**3.14** and **3.16**) were not readily available in our laboratory and so were synthesized for the final synthetic step. This step involved the nucleophilic displacement of the α-bromine to generate the α-aryl substituted 3-indolylethanones (**3.17** – **3.27**).

The thioethers displayed improved antimalarial activity from **2.24** and **2.25** against the chloroquine sensitive 3D7 *Plasmodium falciparum* strain. In addition, these

compounds were non-toxic against HeLa cells which indicated this potential novel class of antimalarials is selective for the malaria parasite as hypothesized in the previous study conducted in our laboratory.

In an attempt to predict the bioavailability of some of our compounds, in silico studies were conducted revealing that these compounds could be passively absorbed by the gastrointestinal tract, a positive result for bioavailability purposes. However, results from these studies indicate that modifications of these compounds would be necessary to allow for permeation through the blood brain barrier (BBB) for instances when the patient has cerebral malaria.

Table of contents

Page

Dedication

“God is in the midst of her; she shall not be shaken.

God will help her when morning dawns.”

- Psalms 46 v 5 –

Dedicated to Godfrey Keirth Chisango (the late), Your Legacy Lives On Daddy!

Acknowledgements

Firstly and most importantly, I would like to thank the Almighty God for His grace, provision, and sustenance throughout this project. I pray that this work will reveal His glory to all who read it and beyond.

I would also like to thank Rhodes University and the National Research Foundation for the financial support they provided for me for this work.

I would like to appreciate and thank my supervisor Dr C.G.L. Veale for the constant encouragement, guidance and support for the last two years. Thank you for seeing the potential in me, and investing time and energy into imparting your special skills and knowledge for my benefit in the laboratory, preparation for the conference as well as the writing of this thesis. I would also like to extend my gratitude to my co-supervisor Dr S.D. Khanye for the unwavering support and advice. May God bless you both abundantly.

I would also like to thank Professor Heinrich Hoppe and Mrs Michelle Isaacs for assisting me with the biological activity assays; Dr R. Tandlich, Mr Borland, Mrs P. Mzangwa for the technical support; and the Faculty of Pharmacy staff members for all the support that made this project a success.

Many thanks to Pastor Innocent, Mama Milcah and the River of Life Church family for the counselling and prayers through the great and tough times I faced through this project. I would also like to thank the Gomwe family and the Zvandasara family for the encouragement and support that kept me going throughout this project.

I also thank my friends and colleagues Faith Magwenzi, Archie Svogie, Lola Oridota, Mayibongwe Lunga, Siyabonga Melamane, Donovan Nel, Carli Weyers and Tiann

Gerwel, Phemelo and Jonathan Hellemann for their support and all the memorable moments we shared together in the laboratory.

Special thanks to Munashe Gomwe for the love and support through every moment of this project. Thank you for the constant motivation. Stay awesome my love!

Lastly, I would like to thank my mother (Grace Chisango) for the sacrifices you made for me to chase my dreams, my sister Linah Chisango for walking this challenging journey with me, my brother Godfrey Chisango for always encouraging me and reminding me of my purpose in this life, the Philip family (Nyasha, Manuel and Kaitlyn) and the Ing family (Kudzai and Vyset) for the unconditional love and going above beyond to do all you could in support of my big dreams. May God bless you all in all your endeavours.

List of Figures

List of schemes

List of tables

List of abbreviations

μM	Micro molar
ºC	Degrees Celsius
^{13}C NMR	Carbon-13 Nuclear Magnetic Resonance
^{1}H NMR	Proton Nuclear Magnetic Resonance
ACTs	Artemisinin-based combined therapy
BBB	Blood brain barrier
BOILED-Egg	Brain Or IntestinaL EstimateD permeation method
COSY	Correlation spectroscopy
Calcd	Calculated
δ	Chemical shift
$CDCl_3$	Chloroform
CH_2Cl_2	Dichloromethane
CH_3NO_2	Nitromethane
CSIR	Council for Scientific and Industrial Research
$CuBr_2$	Copper (II) bromide
d	Doublet
dd	Doublet of doublets
DHFR	Dihydrofolate reductase
DHPS	Dihydropteroate synthase
DMF	*N*,*N*-dimethylformamide
DMSO	Dimethyl sulfoxide
eq.	equivalent
EtOAc	Ethyl acetate
FDA	Food and drug administration
Fig	Figure
GSK	GlaxoSmithKline

h	Hour
HMBC	Heteronuclear multiple bond correlation
HRESMS	High resolution electrospray mass spectrometry
HSQC	Heteronuclear single quantum correlation
HTS	High throughput screening
Hz	Hertz
IC_{50}	50% Inhibitory concentration
J	Spin-spin coupling constant
IPTp	Intermittent preventive treatment in pregnancy
IRS	Indoor residual spraying
ITNs	Insecticide treated nets
IUGR	Intra-uterine growth restriction
K_2CO_3	Potassium carbonate
LDH	Lactate dehydrogenase
LeuRS	Leucyl-tRNA
LLINs	Long lasting insecticidal nets
m	multiplet
m/z	Mass-to-charge ratio
MEF	Murine embryonic fibroblast
MeOD	Deuterated methanol
mg	Milligram
$MgSO_4$	Magnesium sulphate
Min	Minutes
mL	Millilitre
mmol	Millimolar
mp	Melting point
NaH	Sodium hydride

$NaHCO_3$	Sodium hydrogen carbonate
NaOMe	Sodium methoxide
NMR	Nuclear magnetic resonance
NMT	*N*-Myristoyltransferase
PABA	Para-amino benzoic acid
PCR	Polymerase chain reaction
PDE4	Phosphodiesterase type 4
Pf	*Plasmodium falciparum*
$POCl_3$	Phosphoryl chloride
Ppm	Parts per million
Pv	*Plasmodium vivax*
RBCs	Red blood cells
RDT	Rapid diagnostic tests
s	singlet
SAR	Structure activity relationship
sat.	Saturated
$SnCl_4$	Tin (IV) chloride
$SOCl_2$	Thionyl chloride
t	Triplet
TLC	Thin layer chromatography
WHO	World Health Organization

Conference participation

1. Exploring para-thiophenols to expand the structure activity relationship of antimalarial 3-indolylethanones: All Africa Congress on Pharmacology and Pharmacy. “Evidence in Action” 2016.

Chapter One:

Introduction and Literature Review

1.1 General overview: Malaria

The WHO has described malaria as a life threatening, parasitic disease caused by *Plasmodium* pathogens and transmitted by the female Anopheles mosquitoes. The most lethal parasite, *Plasmodium falciparum*, is responsible for the majority of malaria cases in Africa and South East Asia, although *Plasmodium vivax*, and *Plasmodium ovale*, also notably contribute to the morbidity.[1] According to the Centres for Disease Control and Prevention, in 2015, an estimate of 212 million cases of malaria were recorded worldwide resulting in 429,000 mortalities worldwide, the majority of which were children in Africa.[2] However, between 2010 and 2015 the incidence of malaria in high risk populations across all age groups decreased by 21% worldwide, and malaria mortality rates decreased by between 29 and 35% among children under 5.[1] Only a fraction of the people exposed to the malarial parasite in areas of endemic malaria will develop the disease. This is because of key interventions by the WHO after its recommendations were revised in 2012. The recommendations resulted in an increase in the proportion of people with insecticide treated nets (ITNs); an increase in people sleeping under the ITNs; an increase in the proportion of women receiving at least three doses of intermittent preventive treatment in pregnancy (IPTp); by 2014, six of the 15 countries for which the WHO recommends seasonal chemoprevention in children had adopted the policy and

lastly, there has been more diagnostic testing in the public sector followed by treatment, especially in children under the age of 5 with *P. falciparum.* The outcome of this disease is influenced by a variety of factors, including but not limited to the host's genetics, age, nutrition, as well as environmental factors such as transmission rate and the parasitic virulence.[3]

Although there is documented improvement in the mortality rates, malaria has proven itself as a global emergency because decreases in case incidence and mortality rates were slowest in countries that had the largest numbers of malaria cases and deaths.[4] It has been found to affect mostly poor women and children which has resulted in the disease perpetuating a vicious cycle of poverty in the developing world and therefore, more interventions need to be introduced, specifically in developing novel affordable treatment.[5] Pregnant women are particularly at risk. Malaria during pregnancy causes decreased birth weight by intra-uterine growth restriction (IUGR), premature delivery or both.[6] Infection in the first half of pregnancy is associated with a reduction in foetal head diameter[7] while maternal *P. falciparum* malaria changes utero-placental haemodynamics because of the strong association between placental malaria infection and both low birth weight (LBW) and severe maternal anemia.[8] *P. falciparum* infection in pregnancy is usually asymptomatic. However, it often contributes to adverse perinatal outcomes with a high risk for infant mortality, especially in areas that have fewer incidents of malaria. This is because the placenta whose primary purpose is providing sustenance for the developing foetus, is also a site for *P. falciparum* sequestration.[9] This disease along with malaria-related illnesses and mortality cost the African economy USD 12 billion per year.[5]

Malaria is under control in most of Europe, the United States of America and some parts of Asia but remains endemic in many African countries and is a serious problem in many parts of South East Asia.[10] It is not coincidental that the northern and southern tips of Africa have significantly reduced incidents of malaria as they are also home to the richest countries of the continent.[11] Malaria and poverty are intimately connected as it is most prevalent in the poorest countries.[12] It is often referred to as the epidemic of the poor because the impact of malaria is not only felt in terms of the suffering and death experienced by the people, but also the significant economic consequences that result in stunted economic growth as public expenditure costs are directed to the national disease burden.[11] In 2011, 72% of companies in sub-Saharan Africa reported a negative malaria impact with 39% regarding these to be serious as worker productivity decreases with increased sick leave, absenteeism and premature mortality of the workers.[11,13] The world has now reached a critical point in the battle against malaria. Currently, there is both opportunity and an urgent need to hasten progress towards global development goals, by reducing the incidents of malaria and consequently the related deaths in all countries. This can only be achieved by identifying approaches that aim to reduce infection and transmission.[5]

1.2 The life cycle of the parasite

The malaria parasite is complex in its genetic makeup. It develops in both humans for asexual reproduction and in the female *Anopheles*[14] mosquitoes for sexual reproduction and the complexity means that each infection results in thousands of antigens being introduced to the human immune system.[15] The complexity of the malaria parasite comes about from the several life stages it undergoes while in the

human host and thus producing different antigens at different stages of its life cycle as shown in **Figure 1.1**.[16] The malaria infection begins when an infected female *Anopheles* mosquito **Fig 1.1 stage** (**1**) feeds on a human host during a blood meal, injecting the *Plasmodium* parasite into the human's bloodstream in the form of sporozoites. This is the stage of infection.[17]

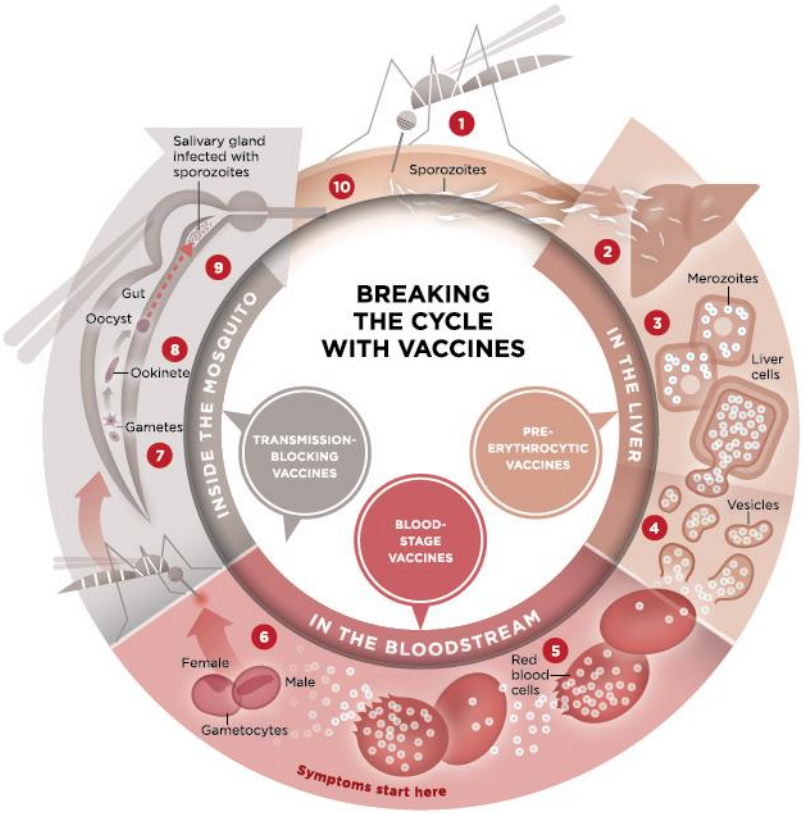

Figure 1.1: Malaria parasite life cycle stages. Image reproduced with permission from site by Allie Mooney[15]

The exoerythrocytic and the erythrocytic phases (the liver and bloodstream phases respectively) are the two different phases of the asexual reproduction stage. The sporozoites travel rapidly to the liver after inoculation, which is their first target (**stage 2**). Once there, they enter the hepatocytes and start dividing into schizonts which give birth to thousands of merozoites (**stage 3**) for each schizont. After 6 – 7 days

the merozoites are released into the blood (**stage 4**), marking the end of the exoerythrocytic stage, where they invade their next target, the red blood cells (RBCs) (**stage 5**), marking the beginning of the erythrocytic phase.[18] For the next 48 hours the merozoites replicate mitotically. The trophozoites formed in the ring stage are unable to digest haem and therefore convert it to haemozoin, but digest the globin moiety that is used as a source of amino acids for their reproduction.[19]

The next cellular stage involves erythrocytic schizont. After each schizont matures, more merozoites are birthed at an average of 16 new daughter merozoites per schizont, and after the RBCs burst they are released into the blood stream to invade more RBCs. It is at this point that the clinical symptoms start manifesting as parasitaemia occurs and the cycles of asexual multiplication continues. The clinical symptoms may include headache, fever and lethargy.[20]

However, some of the infected blood cells leave the cycle and instead of replicating, the merozoites in these blood cells differentiate into male and female sexual forms of the parasite called gametocytes (**stage 6**), that circulate in the blood stream and are non-pathogenic.[19] When a female *Anopheles* mosquito feeds on an infected human host, it ingests the gametocytes during a blood meal which develop further into mature sex cells over a period of time depending on the plasmodium species during a process known as gametogenesis.[15]

The last stage of the sexual cycle occurs in the midgut of mosquito (**stage 7**) where the microgametes (male) and the macrogamete (female) fertilise to form the ookinetes (**stage 8**) that cross through the midgut epithelium and form oocysts on the exterior surface. The oocysts allow for the formation of thousands of active sporozoites and eventually rapture releasing them into the body cavity. These

sporozoites travel (**stage 9**) to the mosquito's salivary glands and a bite into a new human host (**stage 10**) brings the transmission cycle into a full circle.[21]

1.3 Malaria diagnosis

In order to treat the patient in time and to prevent further spread of infection, malaria must be diagnosed promptly and considered a potential medical emergency.[22] This is important for both rapid and effective disease management. The signs and symptoms of malaria are non-specific and cannot reliably be distinguished from any other causes of fever.[18] Diagnosis based on clinical features is not specific and could result in empirical treatment. Therefore for a definitive diagnosis to be made laboratory tests must reveal the presence of the malaria parasite or its components.

Microscopy remains the primary diagnostic tool for malaria in most health care facilities but the quality of microscopy-based diagnosis is frequently inadequate. This involves examining a drop of a patient's blood spread over a slide as a 'blood smear' under a microscope.[20] The sample is previously stained to give the parasites a distinctive appearance under the microscope. Areas that do not have access to microscopy services use the malaria Rapid Diagnostic Tests (RDT).[23,24] This involves the use of a dipstick or cassette format and results are available within minutes. However the accuracy, cost and performance under adverse field conditions needs to be addressed.[25]

Alternative methods include molecular diagnosis which detects parasitic nucleic acid using polymerase chain reaction (PCR). This test is more sensitive than smear microscopy. However, PCR results are not readily available, thereby making the test

useful for confirming the species of malaria parasite after the diagnosis has been made using smear microscopy or RDT.[23]

1. 4 Vector control of malaria

Vector control includes measures directed against a vector of disease, (in this case the mosquito) intended to limit its ability to transmit the disease by protecting areas that are known to promote transmission. The options currently available and being implemented mainly include chemical, biological, natural plant products, and environmental management.[14] Vector control plays a significant role in malaria prevention as it has proven to successfully reduce malaria transmission.[4] However, it has become less effective in recent years due to technical and administrative reasons including poor or failure to adopt alternative methods.[14]

According to the World Health Organization, the two most broadly applicable measures for malaria vector control are long-lasting insecticidal nets (LLINs) and indoor residual spraying (IRS) – spraying residual insecticide on interior walls of homes - as these protect humans from the mosquitoes carrying the malaria parasite.[25,9,26] Vector control in many countries still utilises insecticides in the absence of viable alternatives such as chemoprevention[10] and/or case management which includes prompt diagnosis and treatment of infections.[4] However, this approach has limitations associated with availability of the insecticides as well as the growing resistance of the mosquitoes to the available insecticides.[27]

1. 5 Vaccine control of malaria

Malaria vaccination is aimed at preventing the invasion of erythrocytes by merozoites or to kill the merozoites within the RBCs. The development of a vaccine against the malaria parasite has been met with several challenges as the parasite has a complex life cycle and produces thousands of antigens eliciting different types of immune responses.[28] Vaccination against malaria is considered the most efficient method to prevent this infectious disease.[29] This is because individuals living in areas where there is intense transmission naturally acquire immunity showing that immune protection against malaria can be achieved.[18] Although significant research has gone into the development of a vaccine an effective vaccine is not yet available.[26]

A potential vaccine targeting the pre-erythrocytic stage of the parasite known as RTS,S/AS01 is the most advanced vaccine candidate currently documented.[30,26] It works with the sporozoite as the target and the circumsporozoite protein as the antigen, eliciting a strong immune response.[18] In November 2016 the WHO announced that the RTS,S vaccine would be rolled out in pilot projects in 3 countries in sub-Saharan Africa.[31] In addition over 20 other vaccine constructs are currently being evaluated in clinical trials targeting the liver stage, the merozoites, the blood stage, the toxins and the sexual stages.[18] Although the *Plasmodium* lifecycle is complex, having several targets allows for more opportunities to target the parasite on multiple fronts.[26] Amongst the challenges being faced in the search for a vaccine are high costs associated with vaccine production, along with distribution and delivery.[31]

1.6 Rationale for finding new antimalarial drug

The biggest challenge concerning global malaria elimination is the ability to prevent human-mosquito parasite transmission.[32,33] As mentioned before, strategies that have been implemented include preventing transmission of the malaria parasite by encouraging the use of LLINs and spraying residual insecticide on the interior walls of homes to protect the areas that promote transmission.[25] These strategies, although effective have significant limitations as discussed earlier.[27] Prevention of transmission of the malaria parasite using the LLINs is reduced by washing and low retreatment rates, larval control has been neglected, resistance is building up against IRS insecticides and efforts to develop an effective vaccine have been mostly unsuccessful.[14,16] We therefore need to focus on expanding the selection of chemotherapeutics available to cure infections.[34]

Extensive research has gone into antimalarial drug discovery but due to the occurrence of frequent and widespread drug resistance there still lies an urgent need for new antimalarials.[33] This resistance results in poor management of the disease leading to a significant global health burden. The complex biology of the parasite results in difficulties in identifying compounds that are active against the different life cycle stages of the parasite as each stage has a different target and different antigen involved.[18,35] In addition, the existing antimalarial drugs are either too expensive, toxic or the malarial parasite is developing resistance to them.[36] Amongst the drug candidates for the treatment of malaria according to the WHO treatment guidelines are chloroquine (**1.1**), artemether (**1.2**), artesunate (**1.3**), dihydroartemisinin (**1.4**), lumefantrine (**1.5**), amodiaquine (**1.6**), mefloquine (**1.7**), piperaquine (**1.8**), pyrimethamine (**1.9**) and sulphadoxine (**2.1**).

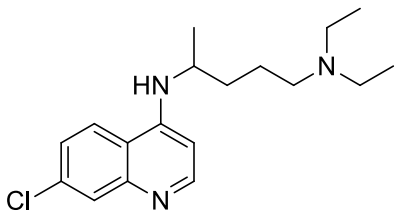

1.1 Chloroquine

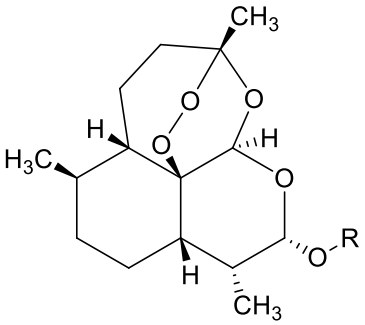

1.2 Artemether: R = Me
1.3 Artesunate: R = -CO-CH_2-CH_2-CO_2
1.4 Dihydroartemisinin: R = H

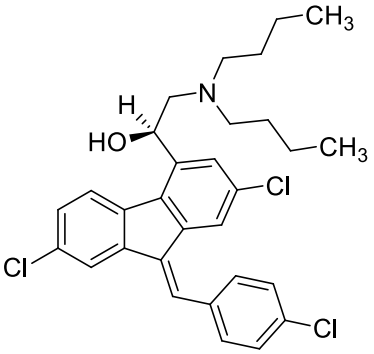

1.5 Lumefantrine

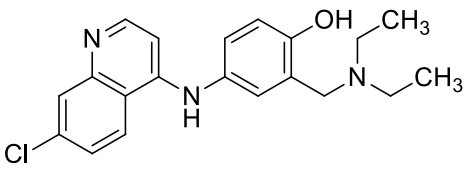

1.6 Amiodaquine

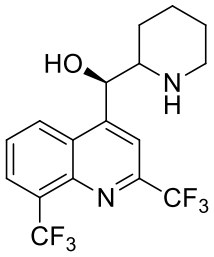

1.7 Mefloquine

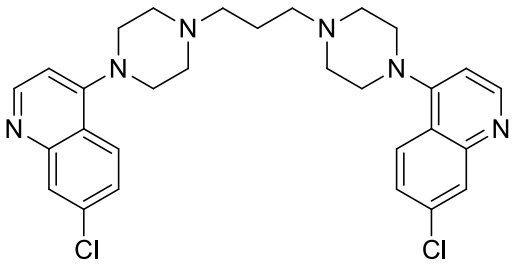

1.8 Piperaquine

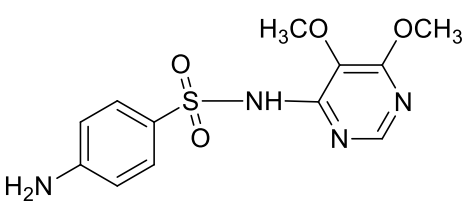

1.9 Sulfadoxine

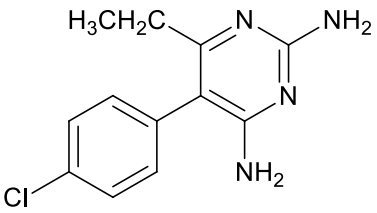

2.1 Pyrimethamine

As early as 2010, partial artemisinin (**1.2 – 1.4**) - resistant *P. falciparum* emerged on the Cambodia - Thailand border and, although unsuccessful, containment strategies were implemented.[37] It has been reported that the malaria parasite is also starting to develop tolerance to the ACTs characterized by prolonged parasite clearance times. Chloroquine (**1.1**) has been the mainstay treatment and control of malaria,[38] however, resistance has resulted from reduced parasitic accumulation of the drug, although the molecular mechanisms responsible have not been fully understood. Amodiaquine (**1.6**) is used in certain areas with minimal chloroquine (**1.1**) resistance as it is reported to be more effective.[39]

The challenge is not only that drug resistance is prevalent; in addition, novel antimalarials need to be fast acting, safe for children and pregnant women, and lastly they should ideally be single-dose administration drugs such as mefloquine (**1.7**) and sulfadoxine (**1.9**) – pyrimethamine (**2.1**) (although all are suffering from resistance).[40] Considering the emergence of drug resistance and the lack of effective antimalarial vaccines it is of great significance to develop novel antimalarial agents for the treatment of malaria.[41] This investigation was prompted by a study conducted by Svogie et al who discovered indolyl-3-ethanone-α-thioethers, a new class of promising antimalarials. Some of the compounds displayed potent nanomolar inhibitory activity in a phenotypic screen against a chloroquine sensitive strain of *P. falciparum* (3D7) without exhibiting cytotoxicity against the HeLa cell line.[42]

Chapter Two:

General overview of anti-malarial drug discovery

2.1 High-throughput screening in antimalarial drug discovery

High Throughput Screening (HTS) is a drug-discovery technique widely used in the pharmaceutical industry and may be applied in biological and chemical sciences.[43] It allows for a large number of drug-like compounds to be assayed against biological targets through the use of automation, miniaturized assays as well as large-scale data analysis.[44] HTS is preferred for its cost-effectiveness, speed, simplicity and high efficiency which means that compounds with poor or no effect can be identified and removed from investigation after a quick scan.[45,46] Although HTS can test hundreds of thousands of compounds in a single day, the cost and time can be further reduced if fewer compounds could be tested without affecting the probability of success of the compounds generated becoming clinical candidates.[47] HTS has proven itself to be a screening tool that is a crucial source of chemical starting points for drug discovery.[44] According to a lecture by Dr Dalu Mancama at the Emerging Researchers Symposium in 2015, the Council for Scientific and Industrial Research (CSIR) has adopted the use of HTS for the screening of thousands of viable compounds that will consequently lead to the permanent disruption of the life-cycle of the malaria parasite, in an attempt to eradicate the disease.[48]

In antimalarial drug discovery, robust and reliable *in vitro* HTS assays are developed to evaluate the effect of a compound on the growth of malaria parasites.[49] Due to

safety, assay stability, cost, equipment availability and quality of data produced, not all of the assay methods are suitable for HTS. The lactate dehydrogenase (LDH) assay, since its description, has been increasingly used for *Plasmodium* growth determination owing to its robustness and specificity.[50]

2.1.1 "Phenotypic" vs target based assay

Phenotypic screens and target-based screens are important strategies that have been adapted for early stage drug development over the last century.[51] Initially, new medicines were discovered by testing different chemicals against phenotypes, the observable characteristics of an organism in biological systems such as animals or cells.[51,52] In general, target-based screens measure the effect of compounds through *in vitro* assays on a purified target protein.[51] For effective target identification, genetic studies need to be guided by good understanding of the target parasites' genetic profile.[34]

Although target-based screens are more efficient because you can target the problem directly, this approach is considered by some as a "reductionist approach" due to the complexity of the biology of human disease and in some instances, might even prove to be more expensive as there will be a need to evaluate multiple hypotheses. This means that identifying a putative target is not sufficient grounds to design a compound unless the target plays a pivotal role to the progression of the disease and can be allowed to proceed for lead optimization.[51,52] Another challenge that is encountered in target-based screening is whether or not the target identified is part of a broader resistance mechanism, such as an efflux pump or an enzyme the disease uses to metabolize the drug and thus countering the activity of the drug.[34]

This method however, has encouraged the use of advances in automation, biochemistry, structural biology and chemistry related technologies to provide efficient and high capacity testing of large numbers of molecular targets and compounds.[53]

Phenotypic screens were the mainstay of drug development and these potentially lead to the identification of a compound that modifies a disease phenotype by either acting simultaneously on more than one target or by acting on a previously unidentified target.[51] Phenotypic approaches use semi-empirical methods and although they do not require an established understanding of the mechanism of action, they do require a basic understanding of the disease biology for appropriate interpretation of data in relation to the disease.[52] Phenotypic assessments are becoming more relevant as the two screening methods work together in drug discovery and newer techniques are incorporated.[54] Guimede et al. released a review on the importance of phenotypic whole-cell screening in malaria drug discovery from the results obtained from HTS programs ran by GlaxoSmithKline (GSK), Novartis and St. Jude Children's Research Hospital that have been released to the public.[34] At GSK, 2 000 000 compounds were screened against intraerythrocytic *P. falciparum*, 19 000 of these compounds were primary hits that inhibited the parasite's growth by more than 80% at 2 μM. At Novartis, a library of natural products were screened *via* HTS and from 12 000 pure compounds, and only 275 were hits. Lastly, the St Jude Children's Research Hospital group screened 300,000 compounds against intraerythrocytic *P. falciparum (3D7 strain)* at a concentration of 7 μM. These compounds were narrowed down to 170 which were selected from the hits from the HTS screen. These results show how whole-cell phenotypic HTS campaigns not only deposits thousands of active compounds into

the public database from both academic and industrial groups but hasten the process of antimalarial drug discovery.[55]

2.2 Medicinal chemistry-based approaches to antimalarial drug discovery

2.2.1 Chloroquine and its derivatives

Medicinal chemistry is a sub-discipline which traditionally focusses on synthetic organic chemistry to drive the identification of novel chemotypes or the optimization of existing drugs. Research in medicinal chemistry involves investigations of drug substances as well as toxic substances and their biological effects with respect to the chemical structures and the respective biological interactions.[56] Chloroquine (**1.1**) was among the first antimalarial compounds synthesised in 1934 by German chemists from synthetic modifications made to quinine (**2.1**), derived from the bark of the cinchona tree, and belongs to a class known as the 4-aminoquinolines (**2.2**).

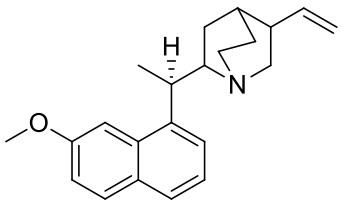

2.1 Quinine

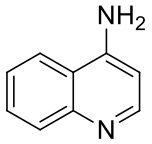

2.2 4-Aminoquinoline

The mechanism of action of 4-aminoquinolines is characterized by the concentration of the drug in the digestive vacuole of the intraerythrocytic parasite.[57] A complex is formed with haem that prevents crystallization in the *Plasmodium* food vacuole. Consequently haem polymerase activity is inhibited, resulting in accumulation of free haem which is cytotoxic to the parasite.[36] Optimal activity of this class is dependent on the terminal amino group which was identified as essential for accumulation, as this is one of the sites where protonation in the digestive vacuole occurs. The

aromatic quinoline moiety also proved useful for the π stacking interactions with the heme protoporphyrin ring and in chloroquine (**1.1**) specifically, the presence of a chlorine atom at the 7-position increased antimalarial activity significantly.[58]

Resistance to chloroquine prompted the research and development of novel quinoline antimalarials such as halofantrine (**2.3**), primaquine (**2.4**), amiodaquine (**1.6**) and mefloquine (**1.7**). Chemical modifications of quinine (**2.1**), resulted in the discovery of these compounds and improved antimalarial activity significantly.[36]

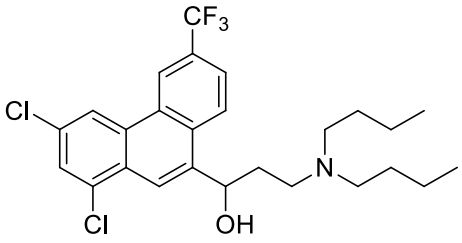

2.3 Halofantrine

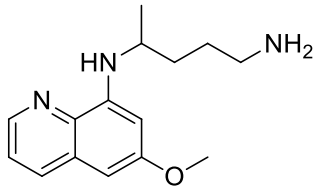

2.4 Primaquine

The anti-malarial agent pyronaridine (**2.5**) is a benzonaphthyridine derivative of mepacrine (**2.6**), one of the earliest synthetic antimalarials.[59] Pyronaridine (**2.5**) was first synthesized in 1970 at the Institute of Chinese Parasitic Disease, Chinese Academy of Preventative Medicine.[60] It is effective against the erythrocytic stage of several species of malaria parasites and the mechanism of action is similar to that of chloroquine. Pyronaridine (**2.5**) inhibits the formation of haemozoin, which leads to disruption of haem detoxification in malaria parasites.[61] Although administered as a single agent in China for over 30 years for the treatment of malaria[60], it is currently used as a partner in artemisinin-based combination therapy (ACT), with artesunate (**1.3**) for the treatment of uncomplicated *P. falciparum* and *P. vivax* malaria in adult and paediatric patients.[61]

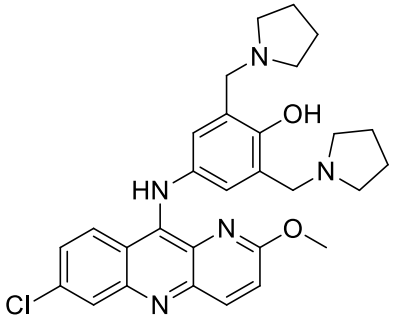

2.5 Pyronaridine

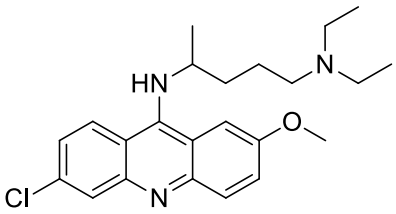

2.6 Mepacrine

2.2.2 Proguanil

Proguanil (**2.7**), a synthetic biguanide derivative of pyrimidine, is a prophylactic antimalarial drug, interest in which grew after the emergence of chloroquine resistance. Cycloguanil (**2.8**), the active metabolite of proguanil (**2.7**), works by halting the reproductive stage of *P. falciparum* and *P. vivax* in red blood cells, by inhibiting the enzyme dihydrofolate reductase (DHFR), which is involved in the reproduction of the parasite.[62] Studies have, however, shown that proguanil also acts as an antimalarial agent in its native form, and when used in combination with atovaquone (**2.9**), a mitochondrial respiratory inhibitor, in the treatment of resistant cases of *P. falciparum* malaria, there was almost 100% efficacy.[62,63]

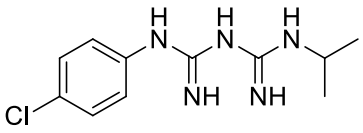

2.7 Proguanil

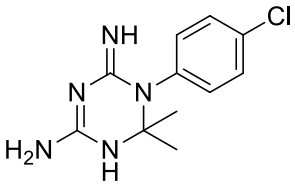

2.8 Cycloguanil

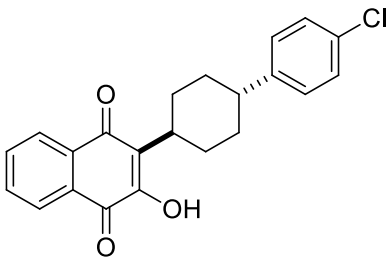

2.9 Atovaquone

2.2.3 Sulfadoxine-pyrimethamine

The success of proguanil (**2.7**) in treating malaria, prompted further study of its chemical class and lead to the development of a new DHFR inhibitor, pyrimethamine (**1.10**).[64] The activity of pyrimethamine is potentiated when combined with the ρ-aminobenzoic acid (PABA) analogue sulfadoxine, a DHPS inhibitor (**1.9**).[65] However, resistance emerged within a year of their discovery and spread quickly in South-East Asia but remained low in Africa until the late 1990s.[64]

2.2.4 Artemisinin and its derivatives

Following the isolation and characterisation of artemisinin (**2.10**) by Chinese scientists in 1972 from *Artemisia annua* several analogues were derived from it by synthetic chemical modification. The 1,2,4-trioxane ring in artemisinin, is the pharmacophore for antimalarial activity of the drug. The endoperoxide bond is cleaved when it comes into contact with iron(II), releasing reactive radicals which

ultimately destroy the parasite. However, the bioavailability of artemisinin was poor for the method of administration (oral) because artemisinin exhibits poor solubility properties in water and oil.[66] Therefore, the necessary synthetic chemical modifications were driven by the desire to improve formulation and bioavailability, by observing the structure-activity relationship (SAR) of artemisin.[66]

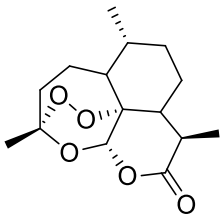

2.10 Artemisinin

The first chemical modifications of artemisinin were on the lactone group which was reduced from the carbonyl with sodium borohydride in methanol to generate the lactol hemi-acetal of dihydroartemisinin (**1.4**) as a mixture of diastereomers resulting in the improvement of the activity of the parent compound but a significant decrease in the stability *in vivo*.[66] Artemether (**1.2**), the lactol ether of dihydroartemisinin (**1.4**), is an oil-soluble derivative and therefore can be administered intramuscularly as well as orally. Through esterification, dihydroartemisinin (**1.4**) was converted into the lactol hemi-ester, artesunate (**1.3**), which is water-soluble and used intravenously for the treatment of advanced cases of malaria.[66,67]

2.2.5 Synthetic Ozonides

Since artemisinin (**2.10**) is a natural product, the production of derivatives is limited to the availability of the plant. In 2004, a completely synthetic peroxide anti-malarial containing a 1,2,4-trioxolane (ozonide) pharmacophore named OZ277 (arterolane) (**2.11**) with anti-malarial activity comparable to that of the artemisinin derivatives was

discovered by Vennerstrom et al.[68] In 2011, arterolane (**2.11**), in combination with piperaquine (**1.8**), was registered for anti-malarial combination therapy in India. The next generation ozonide, OZ439 (artefenomel) (**2.12**), containing a *cis*-8′-phenyl substituent, was more than 50-times more stable to Fe(II)-mediated degradation compared to a first-generation ozonide, such as OZ277 (**2.11**), which contains a *cis*-8′- alkyl group as a result of optimising the structure-activity relationship. OZ439 (**2.12**) shows an increased pharmacokinetic half-life and a good safety profile and is now being tested in phase IIb clinical trials.[69,70]

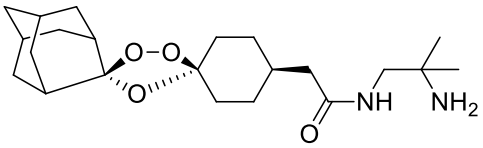

2.11 OZ277

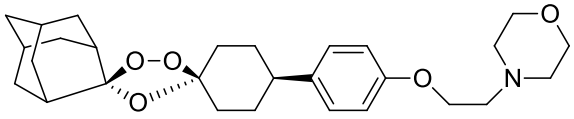

2.12 OZ439

2.2.7 Imidazolopiperazines

Owing to the continuous emergence of parasite resistance, in addition to efforts to modify known pharmacophores, there is an equally important need for the identification of novel antimalarial agents with new mechanisms of action, with activity against multiple stages of the parasite life cycle. This prompted the discovery of a novel class of antimalarial compounds known as the imidazolopiperazines which have potent blood-stage and liver-stage activity.[71] A clinical candidate KAF156 (**2.13**), emerged from lead-optimization of the imidazolopiperazine class.[72] It was identified by high-throughput phenotypic screening, and has potent *in vitro* activity against both asexual and sexual blood stages and the preerythrocytic liver stages of the malarial parasite.[73]

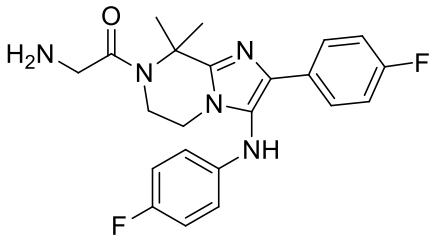

2.13 KAF156

KAF156 (**2.13**) is a promising compound in the Medicines for Malaria Venture's portfolio that has entered phase IIb patient trials in combination with an improved formulation of the existing antimalarial lumefantrine (**1.5**).[72] Compared to other compounds that were being investigated in its class, KAF156 (**2.13**) was selected for its ideal profile which includes a good balance between the desired physicochemical properties required for oral bioavailability, and excellent antimalarial properties.[71] It is the first compound from a novel class of antimalarials which has the potential to rapidly cure malaria infections including resistant strains and blocking transmission of the parasite.[72]

2.2.8 Benzoxaboroles

Very little is known about boron in therapeutics compared to carbon, hydrogen, nitrogen and oxygen. Additionally, there are few boron-containing natural products that medicinal chemists can use as leads. However, the physicochemical and biological properties of boron has allowed for new drug discovery opportunities.[74] Benzoxaboroles (**2.14**) are boron-containing compounds that have proved to be potent against several infectious pathogens, including bacteria, fungi, and trypanosomes.[75] While the exact biological target of this class is unknown, current evidence suggests that they interact with a variety of protein targets including leucyl-

tRNA synthetase (LeuRS) and β-lactamase.[75,76,77] Tavaborole (**2.15**) was the first benzoxaborole to receive FDA approval, an inhibitor of fungal LeuRS, and is used to treat onychomycosis, a fungal infection that cause erosion of the nail plate.[78] Crisaborole (**2.16**), a selective phosphodiesterase type 4 (PDE4) inhibitor, is used in the treatment of atopic dermatitis.[79,80]

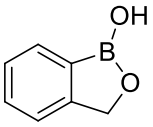

2.14 Benzoxaborole

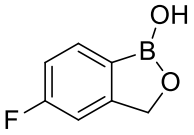

2.15 Tavarole

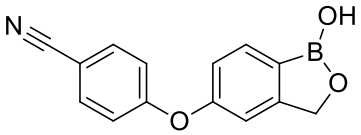

2.16 Crisaborole

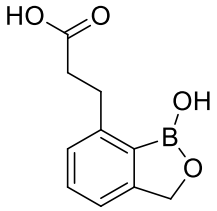

2.17 AN3661

The benzoxaborole AN3661 (**2.17**) has been reported to have potent activity against *P. falciparum* after being screened along with a library of other benzoxaboroles. It has shown minimal cytotoxicity against the mammalian cell lines coupled with activity at nanomolar concentrations. The results of continued investigation into the benzoxaboroles support the continued efforts to add compounds from this class as novel antimalarial agents.[75]

2.2.9 *N*-Myristoyltransferase (NMT)

N-Myristoyltransferase (NMT) is a myristoyl CoA protein that catalyses the addition of myristic acid to the amino-terminal glycine residues of a number of eukaryotic proteins.[81] This enzyme, NMT, has been biochemically characterized, and shown to be significant in *Leishmania major*, *Trypanosoma brucei*, *and T. cruzi*¸ and

proposed as a promising chemotherapeutic target in these trypanosomatids.[82] In addition, NMT has been shown to be an essential and tractable target in malaria parasites both *in vitro* and *in vivo*. It has been observed that selective inhibition of *N*-myristoylation leads to complete and irreversible failure to assemble the inner membrane complex, a pivotal subcellular organelle in the life cycle of the parasite, leading to its subsequent death.[83] The generation of potential development candidates is based on the output of recently reported high-throughput screens. NMT inhibitors for the species *P. falciparum* (Pf) and *P. vivax* (Pv) were screened and **2.18** was found to be a high affinity PvNMT inhibitor with excellent ligand efficiency displaying antiparasitic activity *in vitro* and highlighting a novel binding mode for the scaffold.[84]

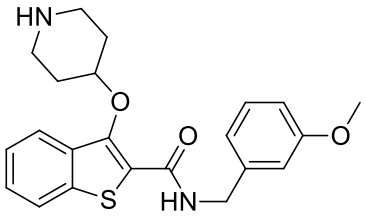

2.18

2.2.10 Synthetic Indoles

The indole nucleus comprises of an aromatic heterocyclic organic compound with a bicyclic structure, consisting of a six-membered benzene ring fused to a five membered nitrogen-containing pyrrole ring.[85] Studies have shown that various indole containing compounds have significant antibacterial, analgesic, anti-inflammatory, anti-pyretic and anti-tumour activity.[86,87] Furthermore, indoles feature in a variety of naturally occurring compounds shown below.[85] Tryptophan (**2.19**) is a natural amino acid, which acts as a biosynthetic precursor for several indolic hormones including

tryptamine (**2.20**), serotonin (**2.21**), and melatonin (**2.22**). Tryptamine (**2.20**) has shown promise for management of anxiety, clinical depression, cluster headaches and substance abuse disorders.[88] Serotonin (**2.21**) is a hormone with vasoconstricting properties, which also plays a part in conducting impulses to the brain, and melatonin (**2.22**) acts as a broad-spectrum antioxidant and free radical scavenger.[89]

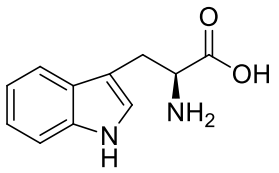

2.19 Trytophan

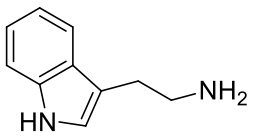

2.20 Tryptamine

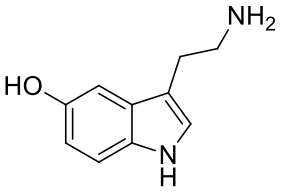

2.21 Serotonin

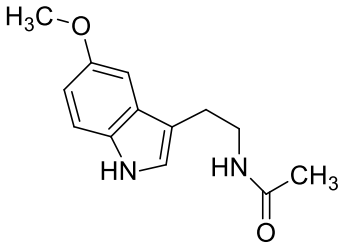

2.22 Melatonin

Due to the fact that the indole moiety and its different analogues are found in many bioactive natural products, this makes them useful tools in drug discovery.[86,87] An investigation by Veale *et al* led to an evaluation of a small cohort of indole ester and amide containing compounds for activity against *P. falciparum*. Biological assessments against a chloroquine-sensitive malarial strain (NF54), a breast cancer cell line (Hs578T) and a non-malignant murine embryonic fibroblast cell line (MEF-1) as a control were conducted using chloroquine, artesunate and paclitaxel were used as control compounds against the cell lines involved. Analysis of the IC_{50} data revealed that one compound (**2.23**) had values in the low micromolar range against

malaria, coupled to significant cytotoxicity against the breast cancer and non-malignant cells.[90]

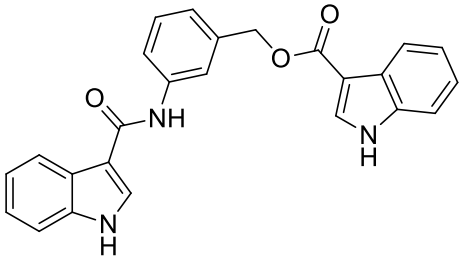

2.23

Svogie *et al* continued the investigation into compound (**2.23**) as a potential antiplasmodial agent in a recent hit identification campaign conducted in our lab.[42] Svogie *et al* discovered two hit thiophenol containing compounds (**2.24** and **2.25**), which were found to have potent and selective antimalarial activity coupled to no observable cytotoxicity against a HeLa cell line. Investigation into the SAR suggested that the para-substituted thiophenyl portion is a key element of the pharmacophore. A nitro substituent in this position resulted in improved activity and when structural modifications were made to the indole, it was noted that the C-5 position also resulted in increased antimalarial activity, coupled to no observable toxicity against a HeLa cell line.[42]

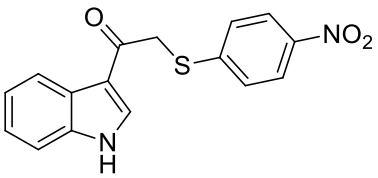

2.24

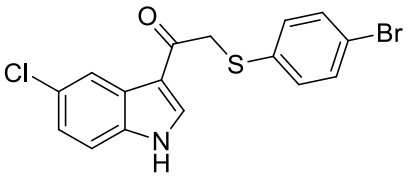

2.25

2.3 Aims and objectives of the thesis

The findings of the Svogie *et al.* investigation provided initial insight into the SAR and a potential pharmacophore of this class of compounds. However, deeper investigation into specific regions was required to fully elucidate the SAR. Accordingly, in this study, we investigated the effect of bioisosteric replacement of the nitro group (a known toxicophore), the phenyl ring, the sulfur atom, the chlorine atom as well as substitution on the indole nitrogen in order to further uncover elements of the pharmacophore of this promising class of antimalarial compounds (**Figure 2.1**). After having synthesized these target compounds, antiplasmodial activity will be determined *via* biological assay and *in silico* analysis. Some of the proposed regions for structural modifications are highlighted below and will be expanded in the remainder of this thesis.

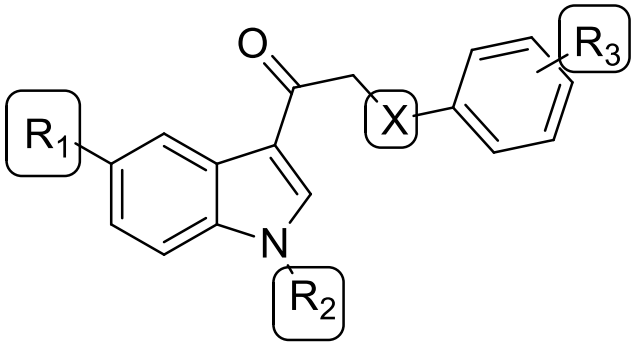

Figure 2.1: Areas for proposed chemical modifications as part of an SAR investigation

Chapter Three:

Results and discussion

3.1 Proposed synthetic pathway

The proposed synthetic pathway illustrated below (**Scheme 3.1**) was adapted from the method developed by Svogie *et al.*[42] In order to expand the SAR from the original study, the target compounds of this study sought to optimize the substituents at positions labelled **R_1, R_2** and **R_3** as per the reasons outlined in the previous chapter, as well as gain further insight as to whether an oxygen or sulfur atom was optimal at position X.

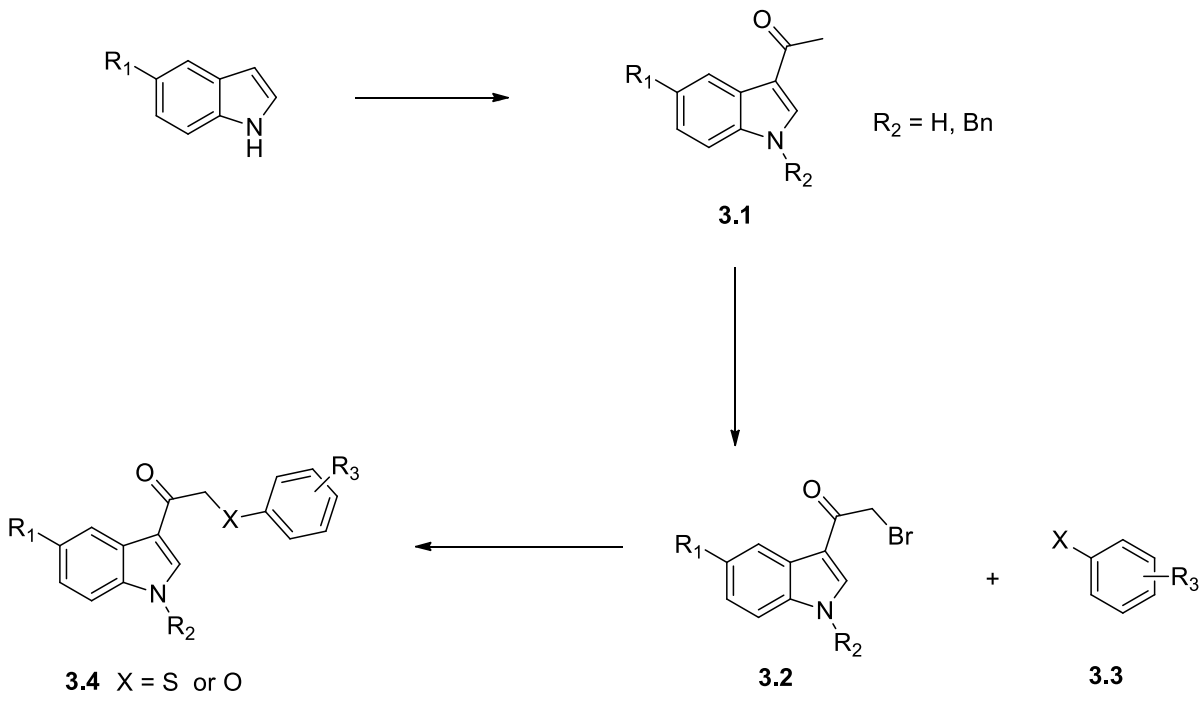

Scheme 3.1 Proposed synthetic pathway

3.2 Synthesis of 3-acetylindoles

As stated in our proposed synthetic pathway (**Scheme 3.1**), our first step involved the synthesis of relevantly substituted 3-acetylindoles. Our lab had previously had success in the application of the modified Friedel-Crafts method of Ottoni *et al.* to indole, which utilises $SnCl_4$ as a Lewis acid and acetyl chloride as a carbon source.[42,91–93] Accordingly, we opted to continue using this method for the purposes of this study, leading to the preparation of our desired 3-acetylindoles **3.5** and **3.6**, respectively, in moderate yield (**Scheme 3.2**).

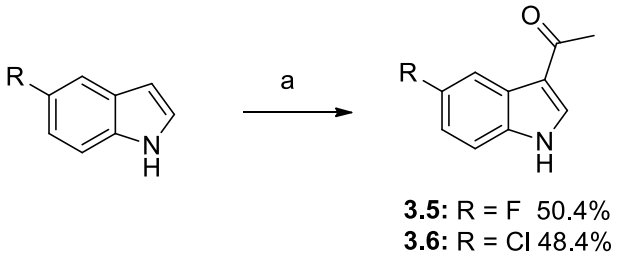

3.5: R = F 50.4%
3.6: R = Cl 48.4%

Scheme 3.2 Synthesis of **3.5** and **3.6**

a) $SnCl_4$, CH_2Cl_2, CH_3NO_2, acetylchloride, N_2, 0 °C - rt, 4 h

3.2.1 Characterisation of compounds 3.5 and 3.6

The success of the acetylation of the substituted indoles was confirmed *via* NMR analysis. For example, the ^{1}H-NMR spectrum of compound **3.6** (**Figure 3.1**), showed a chemical shift at 2.44 ppm integrating for 3 protons, which we attributed to the methyl protons of the acetyl moiety. We also have the assurance that the acetylation did not occur on position 1 due to the presence of the NH signal (12.10 ppm) in the ^{1}H-NMR spectrum. The ^{13}C-NMR spectrum of **3.6** corroborated the ^{1}H-NMR data and showed the characteristic signals for the methyl group (27.6 ppm) and the carbonyl (193.2 ppm). The same characteristic signals were observed in the 5-

fluourinated analogue **3.5**. Furthermore, our NMR spectroscopic data correlated with previous reports.[42]

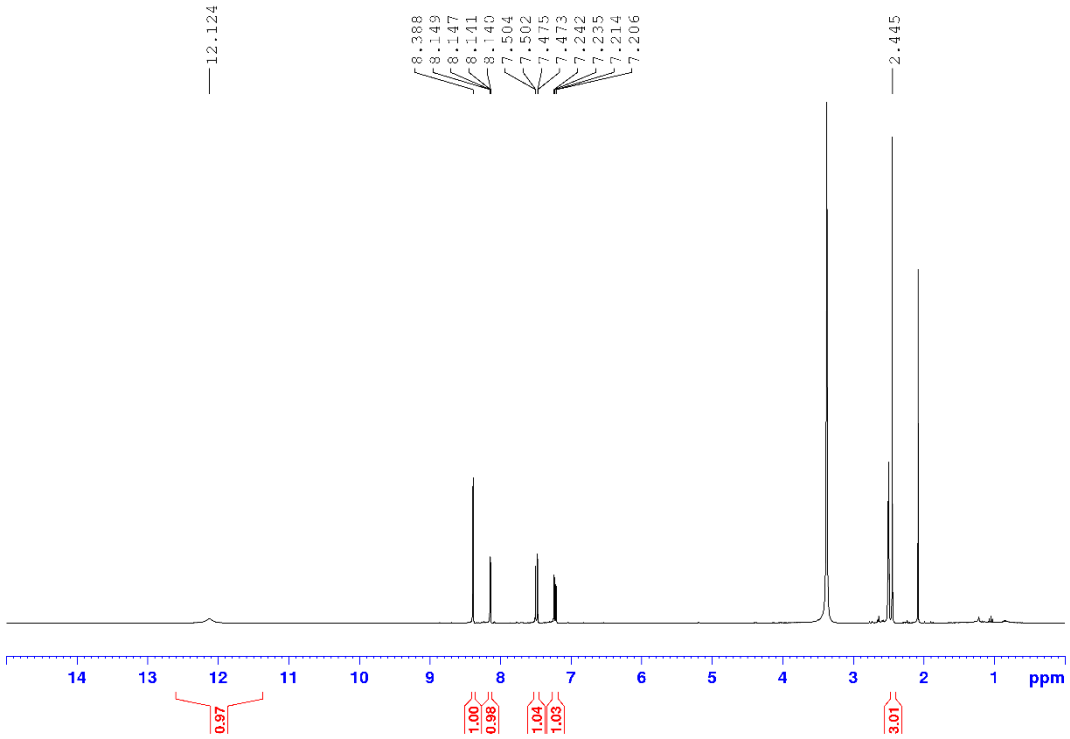

Figure 3.1: ^{1}H-NMR spectrum (300 MHz, DMSO-d_6) for compound **3.6**

3.3 Synthesis of *N*-benzylated 5-chloro-3-acetylindoles

Compound **3.7** was synthesized from compound **3.6**, via benzyl bromide in the presence of NaH in DMF, as per the method reported by Svogie *et al.*[42] (**Scheme 3.3**) in excellent yield.

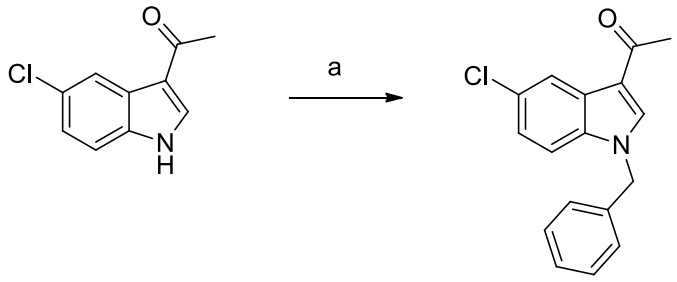

3.6 **3.7** 95.0%

Scheme 3.3 Synthesis of **3.7**

a) DMF, NaH, BnBr, 0 °C, 1 h

3.3.1 Characterisation of compound 3.7

Our initial assessment of the ^{1}H-NMR spectrum of compound **3.7 (Figure 3.2**) suggested that the reaction was successful, due to the absence of the N-H proton signal, as well as presence of a singlet with the chemical shift at 5.51 ppm integrating for 2 protons. Furthermore, additional aromatic signals consistent with the benzyl moiety were observed. Once again, the ^{13}C-NMR spectrum of **3.7** supported the ^{1}H-NMR data and featured the characteristic chemical shift of the benzylic methylene carbon (50.3 ppm). Finally, the NMR spectral data of compound **3.7** corresponded well with previous reports.[42]

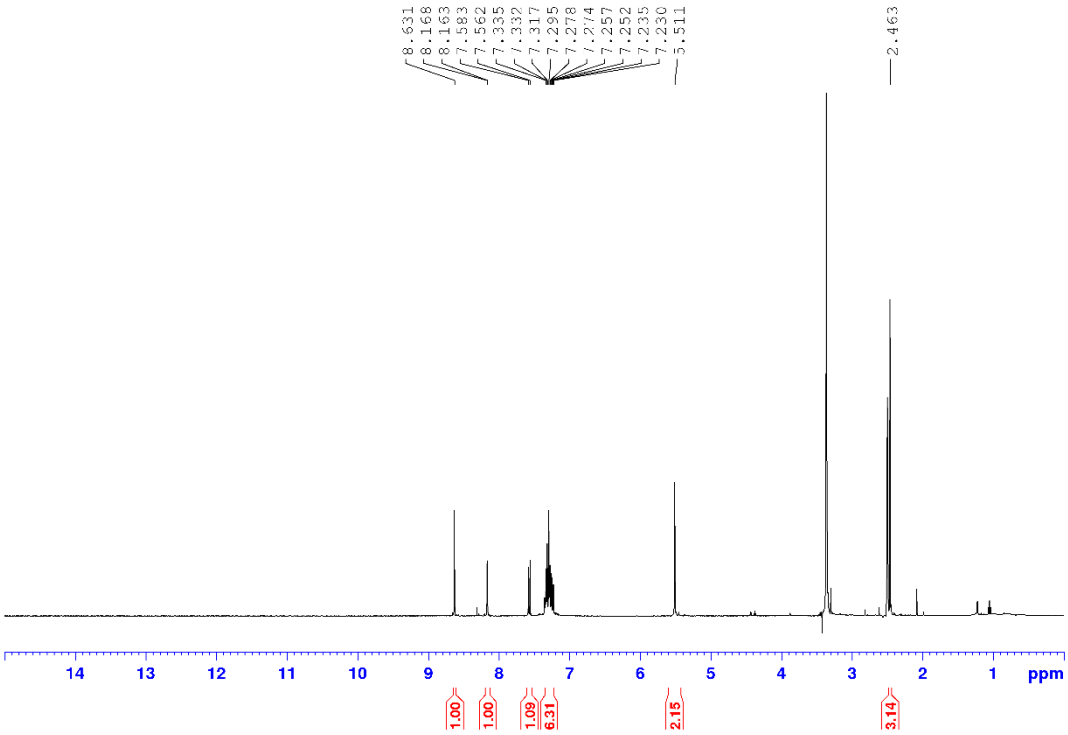

Figure 3.2: ^{1}H-NMR spectrum (400 MHz, DMSO-d_6) for compound **3.7**

3.4 Synthesis of α–brominated 3-acetylindoles

After the successful acetylation of indoles to form the desired 3-acetyl indoles (section **3.2**) followed by the *N*-benzylation of **3.6** (section **3.3**) we proceeded to the selective bromination step to generate the desired α-bromo carbonyl intermediates (**3.8 – 3.11**, **Scheme 3.4**). Owing to our groups' experience of this reaction, we opted to continue using the bromination method reported by King *et al.*, utilising $CuBr_2$ as the brominating agent,[94] which we have modified for our purposes.[92] In addition to the three synthetically derived 3-acetyl indoles, the unsubstituted 3-acetylindole was readily available in our lab for the bromination step.

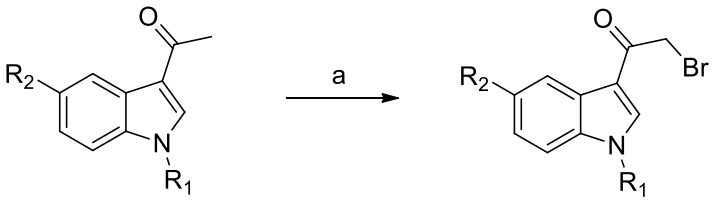

3.8: R_1 = H, R_2 = F 33.5%
3.9: R_1 = H, R_2 = H 51.6%
3.10: R_1 = H, R_2 = Cl 35.6%
3.11: R_1 = Bn, R_2 = Cl 92 %

Scheme 3.4 Selective α-bromination 3-acetylindoles
a) $CuBr_2$, $CHCl_3$, EtOAc, reflux, various times

The α-bromination of 3-acetyl indoles with $CuBr_2$ resulted in the formation of the desired α-bromo carbonyl compounds albeit in low to moderate yield for compounds **3.8 – 3.10**. This method suffers from one major drawback, whereby a second bromination occurs at the α-position, following the initial formation of the desired product.[92] Unfortunately, this side product could not be used in the next step of our synthesis. In addition, the dibromination cannot be reversed, meaning the starting material cannot be recycled. Furthermore, the rate at which the side product forms is seemingly unique to each reaction substrate.[92] Accordingly each of these reactions were monitored constantly by TLC, and halted upon the first indication that the side product started to form. Unreacted 3-acetyl indole was recovered and the reactions repeated, allowing us to accumulate sufficient quantities of α-bromoketones to proceed to the next step of our study.

3.4.1 Characterisation of compounds 3.8 – 3.11

To illustrate the successful formation of our desired target α-bromoketones, the ^{1}H-NMR spectrum of compound **3.10** is shown below (**Figure 3.3**). In this spectrum, we

observed a new singlet at 4.54 ppm integrating for 2 protons, and the absence of the methyl ketone signal, which correlates with the conversion of the CH_3 group to a CH_2 after the successful bromination. In addition, the ^{13}C NMR spectrum featured the characteristic signals of the CH_2 (33.8 ppm) functionality in addition to the carbonyl shift (186.9 ppm) confirming our successful synthesis of α-bromo carbonyl compounds.

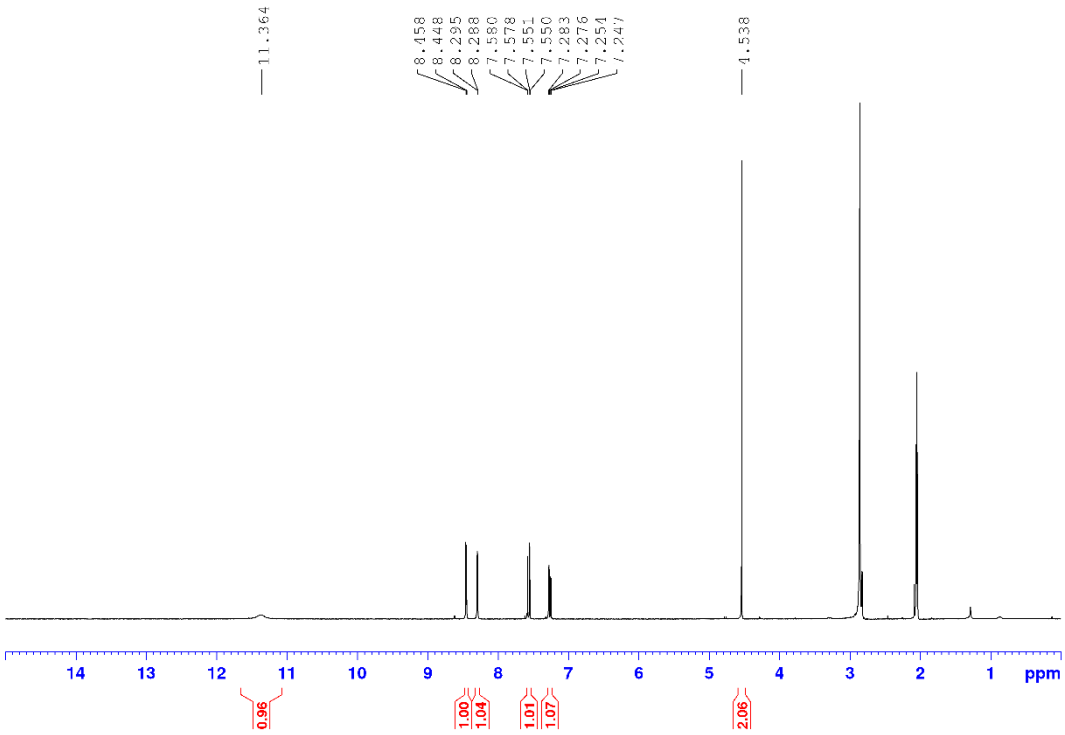

Figure 3.3: ^{1}H-NMR spectrum (300 MHz, Acetone-d_6) for compound **3.10**

3.5 Synthesis of desired thiophenols

As stated previously, this study sought to expand the antimalarial SAR of compounds described by Svogie *et al*.[42] Accordingly, we were interested in bioisosterically replacing the para-substituted nitro group of the thiophenol, with

electron withdrawing groups. Specifically, we were interested in a carboxylic acid, its methyl ester and an amide, which occupy a similar chemical space and orientation to a nitro group. In addition, we were interested in a strongly electron withdrawing nitrile group. Conveniently, 4-mercaptobenzoic acid (**3.13**) was commercially available. We therefore resolved to convert the acid into an acid chloride, which would then allow for nucleophilic displacement of the chloride with either sodium methoxide or ammonia to yield the ester and amide respectively. 4-Phenoxybenzoic acid was used as a model substrate (**Scheme 3.5**), which yielded compound **3.12** in good yield.

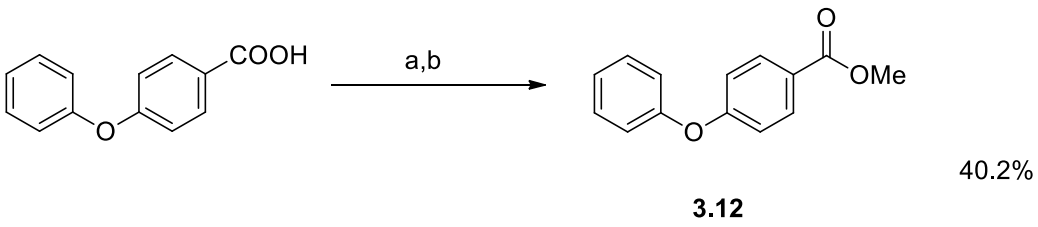

Scheme 3.5 Synthesis of methyl ester **3.12**

a) $SOCl_2$, 70 °C, 2 h; b) NaOMe

We then successfully applied this method to the synthesis of ester **3.14**, and a slightly modified method to the synthesis of amide **3.15**, in poor yields. Finally, we generated the para-cyano thiophenol (**3.16**), through the $POCl_3$ mediated dehydration of **3.15**.

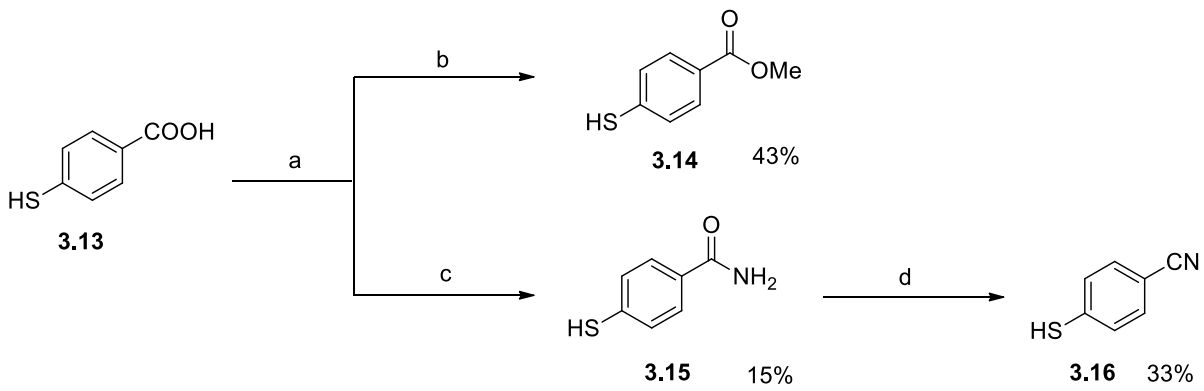

Scheme 3.6 Synthesis of additional thiophenol analogues

a) $SOCl_2$, 70 °C, 2 h; b) NaOMe ; c), NH_3, 75 °C, 2 min d) DMF, $POCl_3$, 0 °C, 2 h

3.5.1 Characterisation of compounds

To illustrate the successful formation of our desired thiophenol analogues, the ^{1}H-NMR spectrum of **3.14** and ^{13}C NMR spectra of **3.16** are shown below (**Figure 3.4** and **3.5**, respectively). In the ^{1}H-NMR spectrum of **3.14** (**Figure 3.4**), we observed a new chemical shift at 3.82 ppm integrating for 3 protons which correlates with the addition of the methoxy moiety. **Figure 3.5** shows the ^{13}C NMR spectrum of **3.16**, which features an additional carbon signal, the characteristic signal of the CN functionality at 118.4 ppm.

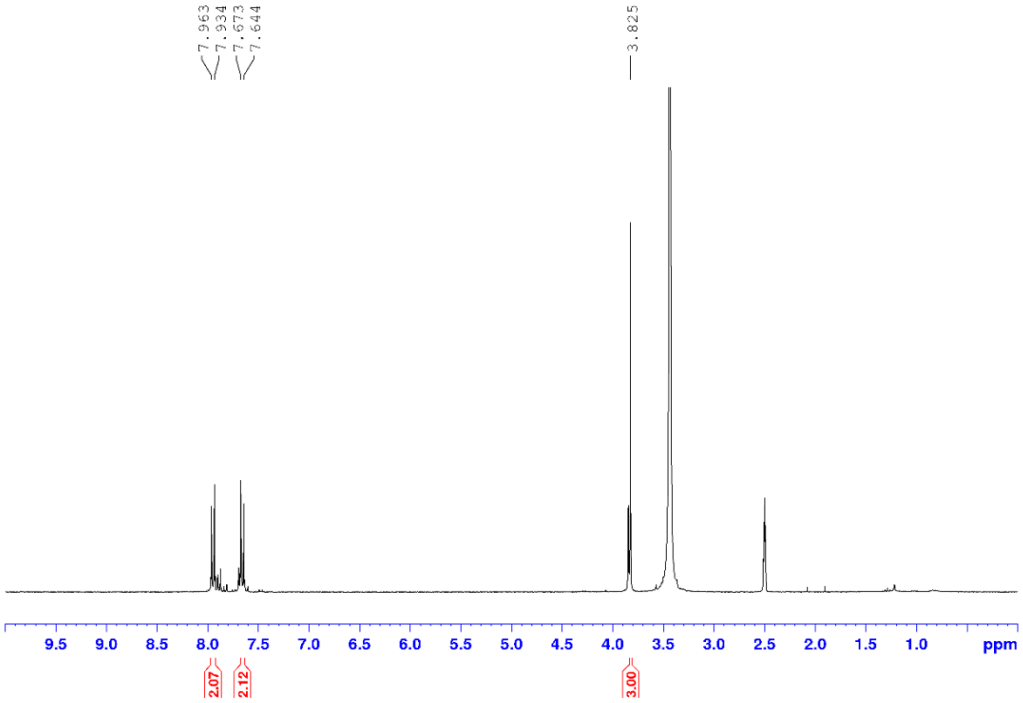

Figure 3.4: ^{1}H-NMR spectrum (300 MHz, DMSO-d_6) for compound **3.14**

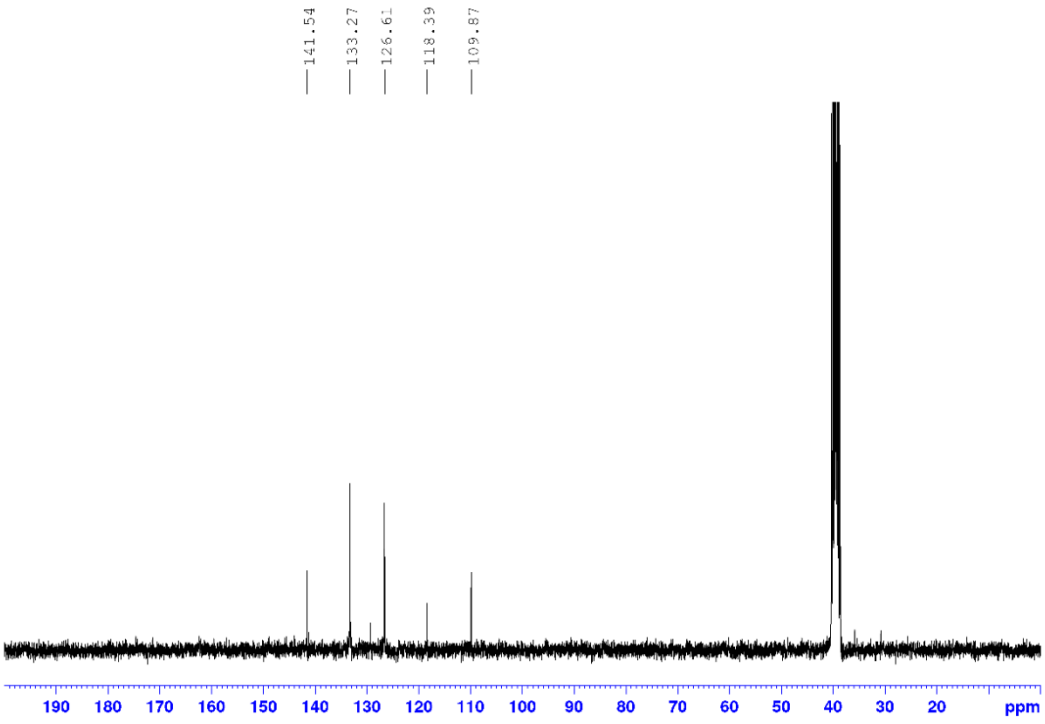

Figure 3.5: ^{13}C NMR spectrum (75 MHz, DMSO-d_6) for compound **3.16**

3.6 Nucleophilic displacement of α-bromine to generate α-aryl substituted 3-indolylethanones

Having installed the good leaving group at the position α to the carbonyl position, the final step in our synthetic procedure involved nucleophilic displacement with a series of phenols and thiophenols in order to generate our desired series of compounds, following the general procedure (**Scheme 3.6**) as described by He *et al.*[95] In addition to the thiophenols to be synthesised, numerous phenols and thiophenols of interest were commercially available.

While the majority of reactions proceeded relatively smoothly, after several attempts to synthesize target compounds **3.13a** and **3.15a** using 4-mercaptobenzoic acid (**3.13**), and 4-mercaptobenzamide (**3.15**) respectively, we were unable to recover any desired products, whose formation was suggested by TLC plates, following flash chromatography. We attributed this to the relatively high polarity of the phenyl substituents, which resulted in attractive forces between the compounds and the silica. The yields attained for the final compounds are tabulated as shown in **table 3.1**. Compounds **3.19**, **3.21**, **3.22** and **3.27** had relatively low yields even after extended reaction times. The low isolated yield can possibly be explained by the fact that the last step of the synthetic pathway was ran on a smaller scale. This came about as a result of losing material over the other steps through the purification process and thus loading a small mass on silica for purification resulted in low yields. The thiophenol used for the synthesis of compound **3.21** and **3.27** was difficult to synthesize which resulted in a small scale reaction for the final synthetic step. Conversely, compounds **3.23** and **3.25** had relatively high yields because the

nucleophiles were readily available and the last synthetic step could be ran on a higher scale which resulted in the ease of purification *via* flash chromatography.

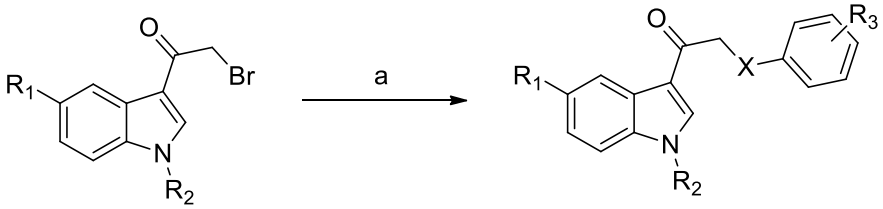

Scheme 3.6 Synthesis of **3.17 - 3.27**

a) O, S nucleophile, K_2CO_3, acetone, reflux, 5 h

3.6.1 Characterisation of compounds 3.17 – 3.27

Standard analytical techniques were used to characterize compounds **3.17 – 3.27.** The ^{1}H-NMR spectra of these compounds showed signals for the indole scaffold, additional aromatic protons from the introduction of substituted phenols and thiophenols, as well as the diagnostic CH_2, all of which integrated to the correct proportion. For example, in the ^{1}H-NMR spectrum of **3.17** the *para*-bromo thiophenyl protons feature as doublets in addition to the pre-existing indole signals in the aromatic region of the spectrum (**Figure 3.6**). The complete structural elucidation for each of the α-aryl substituted 3-indolylethanones (i.e. **3.17** – **3.27**) was done *via* 2D NMR data sets consisting of COSY, HSQC and HMBC spectra. High resolution mass spectra, melting points and IR spectra were also obtained for all final compounds and are included in the experimental chapter.

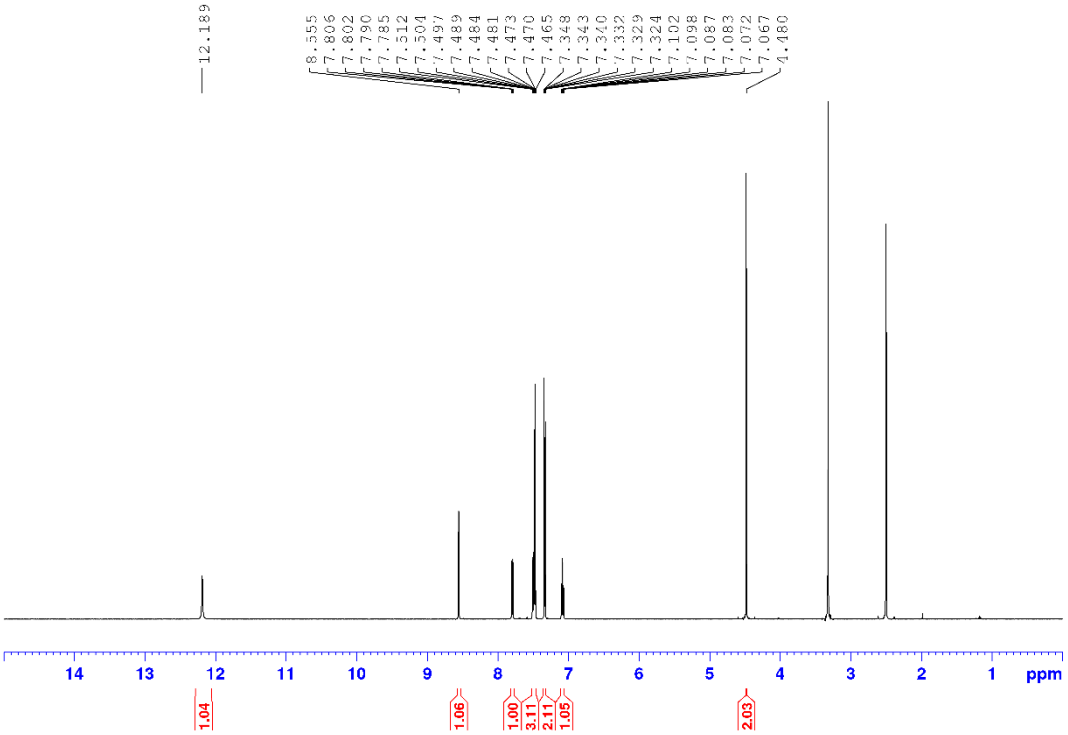

Figure 3.6: ^{1}H-NMR spectrum (600 MHz, DMSO-d_6) for compound **3.17**

Table 3.1: Compounds 3.13a - 3.27 and percentage yields

Compound number	Structure	Yield (%)	Compound number	Structure	Yield (%)
3.13a	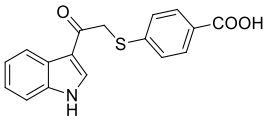	0	**3.22**	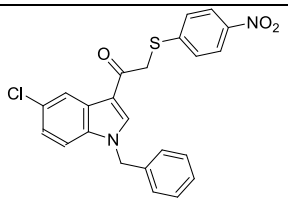	20
3.15a	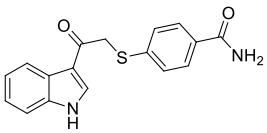	0	**3.23**	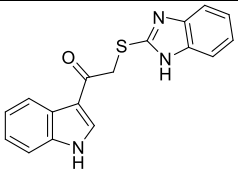	73
3.17	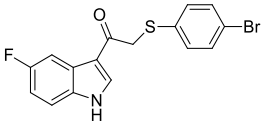	62	**3.24**	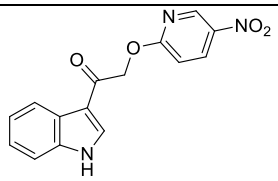	12
3.18	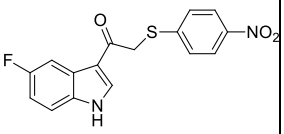	54	**3.25**	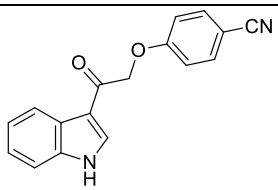	75
3.19	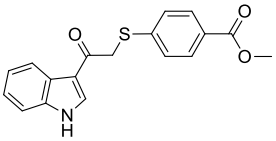	25	**3.26**	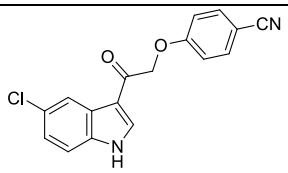	35
3.20	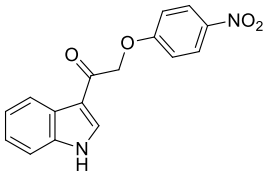	66	**3.27**	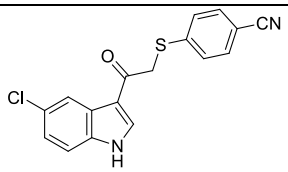	35
3.21	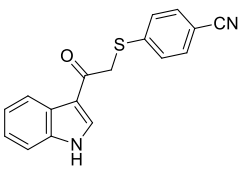	22			

3.7 Biological Evaluation and Discussion

Our investigations were based on SAR optimisation which involved the modification of new chemical compounds and evaluating the consequent biological effects. Similar compounds may display different biological effects and therefore need to be refined until the optimal structure for the desired biological results is obtained.

Table 3.2: Single concentration inhibition, % HeLa cell viability at 20 μM and growth inhibition assays for compounds 3.17 – 3.27

Compound no.	Structure	% Parasite viability at 20 μM	% HeLa cell viability at 20 μM	IC_{50} (μM) 3D7	pIC_{50}
2.24	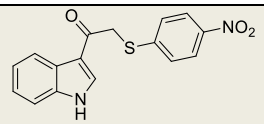	–	–	0.24	6.6
2.25	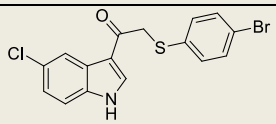	–	–	0.09	7.0
3.17	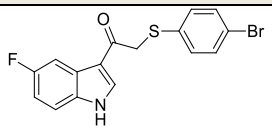	3.03	83.8	1.1	5.9
3.18	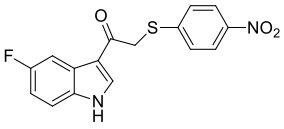	1.36	80.4	0.098	6.9
3.19	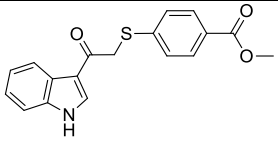	0.620	88.6	2.5	4.5
3.20	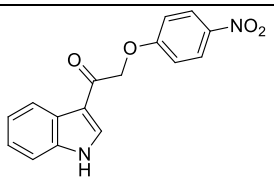	-3.17	76.8	0.46	6.4

3.21	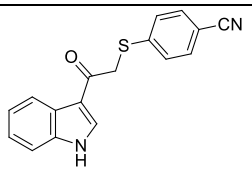	14.2	91.1	0.13	6.8
3.22	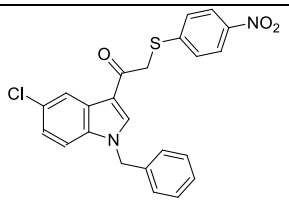	109	n/a	n/a	n/a
3.23	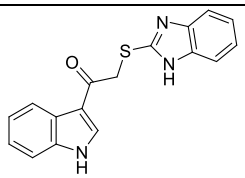	120	n/a	n/a	n/a
3.24	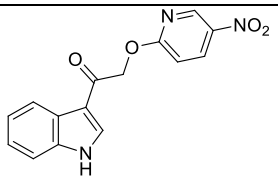	83.9	88.8	n/a	n/a
3.25	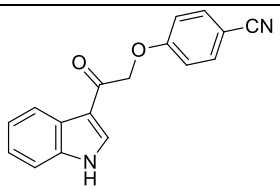	44.2	n/a	0.41	6.3
3.26	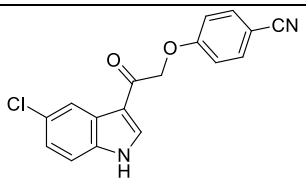	18.5	98.9	0.10	6.9
3.27	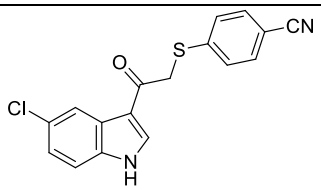	11.5	79.1	0.028	7.5

Svogie *et al.*[42] identified two hit thiophenol containing compounds (**2.24** and **2.25**) which provided the initial insight into the potential pharmacophore of this class of compounds. Having successfully synthesized the small cohort of desired compounds (**3.17 – 3.27**) they were submitted for whole cell phenotypic biological evaluation

against *Trypanosoma brucei* (data not shown) as well as a chloroquine-sensitive *P. falciparum* (3D7) strain. A HeLa cervical cancer cell line was used as a control for mammalian cytotoxicity. Each compound was initially assayed at a single concentration (20 µM). Any compounds which caused cell viability to drop below 25% were taken forward for dose dependant growth inhibition studies to render an IC_{50} value. Conversely, any compound which did not reduce cell viability below this threshold at 20 µM was considered inactive, and excluded from furthered assessment (**3.22** – **3.24**). Interestingly, while several compounds showed encouraging single concentration inhibitory data against *P. falciparum* (**Table 3.1**) none of the compounds assessed in this study significantly inhibited *T. brucei* or HeLa cell viability at 20 µM, indicating that the mechanism of action of these compounds may well be selective to malaria.

In addition to representing our dose dependant data as IC_{50} values, in our data analysis, we opted to use pIC_{50} (the negative log of the IC_{50} value in molar) as well. IC_{50} curves are calculated as a log function, which implies that comparison of data in this format will be more robust. Furthermore, contemporary opinion suggests that interpretation of an SAR from pIC_{50} data will provide a simpler assessment of relative potencies of compounds. Finally, multiple pIC_{50} values from the same compound can be averaged, whereas normal IC_{50} values cannot.[96]

When the unsubstituted compounds **3.19** – **3.21** were assessed, the methyl ester in compound **3.19** resulted in a marked reduction in activity. The substitution of the sulphur moiety with an α oxygen atom for compound **3.20** indicated a decrease in activity when compared to compound **2.24** synthesized by Svogie *et al*.[42] This suggests that the α-sulphur atom is an important element of the pharmacophore

which is compromised by the α-oxygen atom when introduced. We discovered that introduction of a nitrogen into the phenyl portion of the molecule was detrimental to activity, as was replacing the thiophenyl with a benzimidazole. Consequently, we decided that a heterocyclic ring was not necessary for an improvement in activity as shown in the pIC50 results for compounds **3.23** and **3.24**, and therefore we did not explore pyridine or imidazole in compounds with substituted indoles. Importantly, the replacement of the nitro moiety (**2.24**) with a nitrile substituent (**3.21**) resulted in improved activity, which we felt could be further optimized.

Svogie *et a.l*[42] discovered that substitution at position 5 of the indole with a chlorine atom resulted in the best activity in their series coupled to no cytotoxicity.[42] Bioisosteric replacement of the chlorine atom with a fluorine atom resulted in good activity for compounds **3.17** and **3.18**. However, it was noted that activity was lowered when there was a fluorine atom in the C-5 position as opposed to when there was a chlorine atom. This was attributed to the size of the halogen which appeared to influence activity.

Accordingly, compound **3.26** was synthesized with the chlorine atom on the C–5 position, an α-oxygen atom, and the nitrile in the *para* position. The pIC50 for this compound was 6.98. Replacement of the oxygen with an α-sulfur atom, resulted in the most active compound of the series (**3.27)**. While the nitro is strongly electron-withdrawing and rarely found in nature, the nitrile is used in several pharmaceutical products, has good solubility properties, and decreases susceptibility to oxidative metabolism in the liver.[97]

The *N*-modification for compound **3.22** did not result in increased activity so further modification was not necessary. This position was explored to check if there was a

possible binding pocket in that region so as to optimize the compound. However, it was noted that benzylation resulted in decreased activity as the compound did not reduce cell viability at 20 μM as shown in **table 3.1**. This also suggested that the NH is important for activity, possibly due to the H-bond donating effect.

3.7.1 *In silico* comparison of BBB and intestinal absorption of 3.26 and 3.27

Below is a diagrammatic representation known as a BOILED-Egg (Brain Or IntestinaL EstimateD permeation method) for compounds **3.26** and **3.27**. It shows the proposed gastrointestinal absorption and brain penetration of small molecules by computing their lipophilicity and polarity which will be useful information to be able to predict bioavailability.[98] In cases where a patient has cerebral malaria, treatment needs to be available that can penetrate the BBB. Therefore, certain modifications are necessary to improve absorption but still maintain or improve antiplasmodial activity.

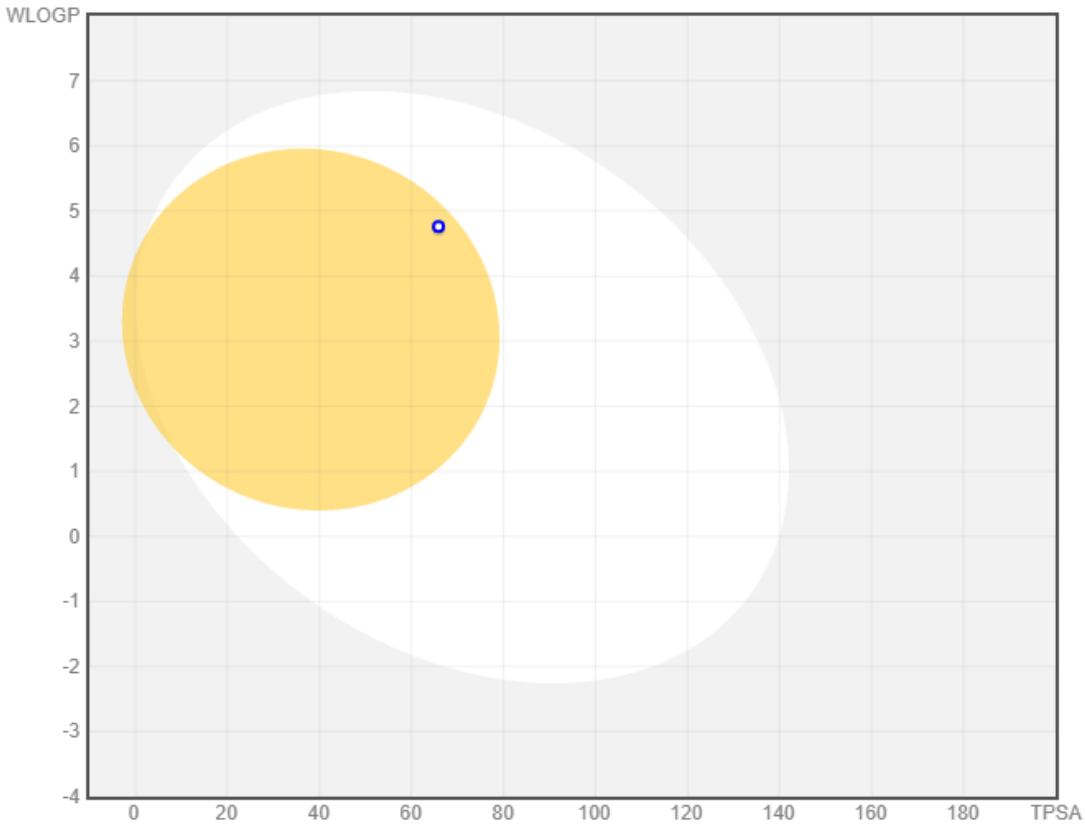

Figure 3.7: BOILED-Egg diagrammatic representation for compound **3.26**

The points located in the BOILED-Egg's yolk are molecules predicted to passively permeate through the blood-brain barrier. Points located in the BOILED-Egg's white are molecules predicted to be passively absorbed by the gastrointestinal tract.[98] In **Figure 3.7**, our diagram shows that our compound **3.26**, illustrated by the blue spot, located in the BOILED-Egg's yolk will passively permeate the BBB, a positive result for our studies for bioavailability purposes. In comparison, **Figure 3.8** which shows the BOILED-Egg diagrammatic representation for compound **3.27**, the red spot located in the BOILED-Egg's white indicates that this compound will only be passively absorbed by the gastrointestinal tract. Although the oxygen seemingly improves BBB absorption it decreases the anti-plasmodial activity.

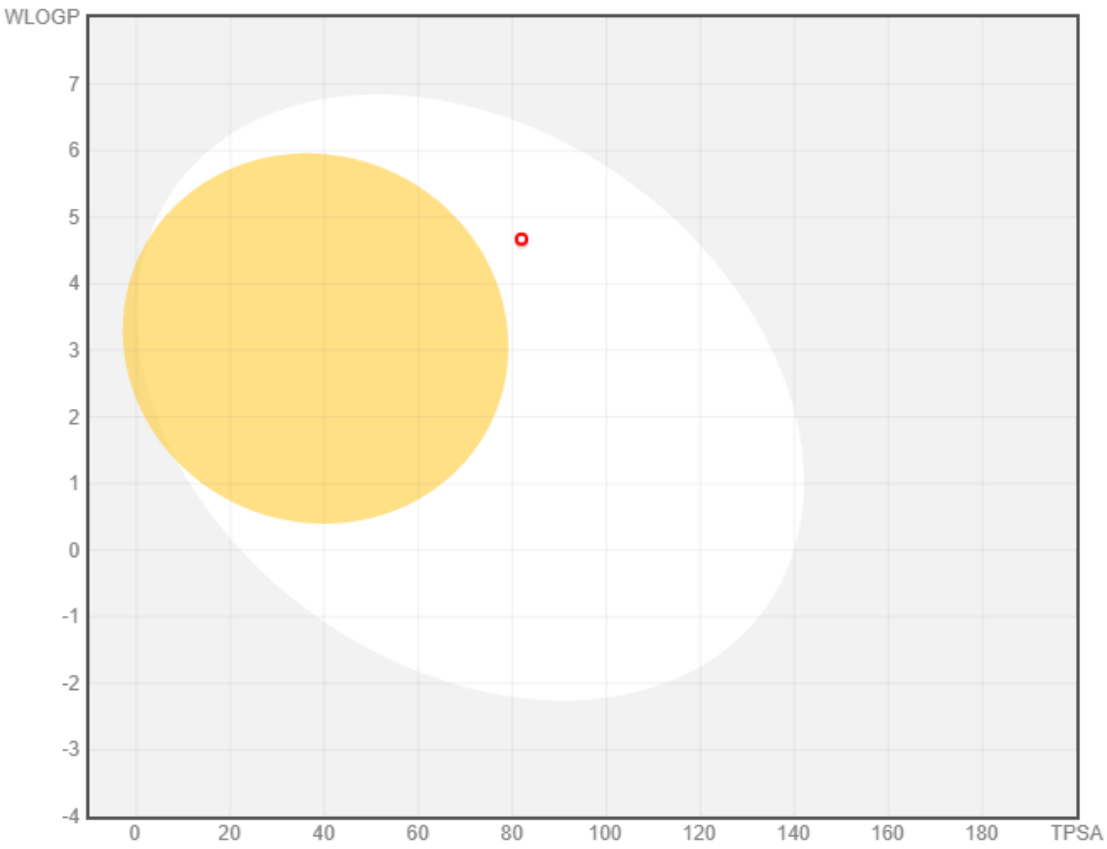

Figure 3.8: BOILED Egg diagrammatic representation for compound **3.27**

3.8 Conclusion

In conclusion, we were able to synthesise our target compounds in low to moderate yields. Our synthetic route involved a three-step method that started with the acetylation of the indole when 3-acetyl indoles were not available (**section 3.2**). After a purification process, the next step was selective bromination (**section 3.4**), which was followed by the coupling step with our phenols and thiophenols (**3.17 – 3.27**), some of which we synthesised (**section 3.5**) if the nucleophile was not readily available to us.

This investigation showed us that the chlorinated C-5 position with a chlorine atom was important for activity as illustrated by compound **3.17** when compared to results obtained by Svogie *et al*.[42] We also discovered that *N*-modification (compound **3.22**) is not necessary and the α-sulfur atom was concluded to be preferable over the α-oxygen atom. Modification of the phenyl ring, although it resulted in no cytotoxicity for compounds **3.23** and **3.24**, there was no significant activity against the 3D7 strain. It was noted that the *para* position was important for activity when there was a nitro substituent,[42] and due to the fact that a nitro is a known toxicophore, bioisosteric replacement led to the discovery of the hit compound **3.27**. The BOILED-Egg diagram in **Figure 3.8** also showed a positive result for absorption in the gastrointestinal tract with the need for further modification for BBB penetration.[98]

Chapter Four:

4.1 Chemistry and experimental procedures

4.1.1 General Chemistry

NMR spectra were acquired on either a Bruker Fourier 300 MHz, or a 600 MHz Avance II spectrometer. Chemical shifts are reported in ppm, referenced to residual solvent resonances (MeOD, δ_H 3.31, δ_C 49.00 ppm; Acetone, δ_H 2.09, δ_C 205.87 ppm; $CDCl_3$, δ_H 7.26, δ_C 77.0; DMSO-d_6 δ_H 2.50, δ_C 39.50 ppm).[99] High resolution mass spectrometry was performed on a Waters Synapt G2 TOF instrument with an ESI source. Flash chromatography was performed using Kieselgel 60 (230–400 mesh) silica gel. Anhydrous solvents were prepared by standard procedures outlined by Perrin and Armarego [100] as well as Casey, Leonard, Lygo and Procter.[101] Infrared spectra were recorded on a Perkin Elmer Spectrum 2000 FT-IR. Melting points were determined using an SMP30 Advanced Digital Melting Point machine.

4.1.2 General procedure for the synthesis of 3-acetylindoles 3.5 and 3.6:

$SnCl_4$ (0.520 mL, 1.2 eq.) was added to a stirred solution of indole (3.70 mmol, 1 eq.) in dry CH_2Cl_2 (7.5 mL) under argon at 0 °C after which the ice bath was removed. After stirring for a further 30 min, acetyl chloride (1.2 eq.) was added dropwise to the reaction suspension, followed by CH_3NO_2 (4.5 mL). The reaction was quenched with ice and water after 4 h and extracted with EtOAc (100 mL). The organic fraction was

washed with water (2 × 20 mL), sat. brine (2 × 30 mL) and dried over anhydrous $MgSO_4$. Solvent was removed *in vacuo* followed by purification *via* normal phase flash chromatography (100% CH_2Cl_2). *In vacuo* solvent removal afforded a brown tarry solid which was dissolved in cold acetone and allowed to evaporate slowly. The resultant crystals were washed with cold chloroform to yield the desired product.

1-(5-Fluoro-1*H*-indol-3-yl)ethanone (3.5):

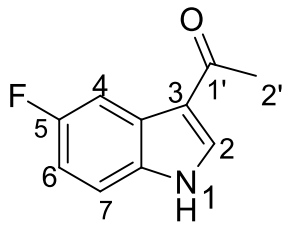

Yield = 50%; **^{1}H NMR (DMSO, 300 MHz)**: δ_H 12.01 (s, 1H, NH-1); 8.36 (s, 1H, H-2); 7.86 – 7.79 (dd, 1H, H-4, J_1 = 8.9 Hz , J_2 = 2.34 Hz); 7.50 – 7.45 (m, 1H, H-7); 7.10 – 7.02 (m, 1H, H-6); 2.44 (s, 3H, H-2') ppm; **^{13}C NMR (DMSO, 75 MHz))**: δ_C 193.1 (q_c, C-1'); 160.6 (q_c, C-5); 136.3 (CH, C-2); 133.6 (q_c, C-7a); 126.3 (q_c, d, $J_{F.C}$ = 11.2 Hz, C-3a); 117.3 (q_c, d, $J_{F.C}$ = 4.4 Hz, C-3); 113.9 (CH, d, $J_{F.C}$ = 10.5 Hz, C-7); 111.5 (CH, d, $J_{F.C}$ = 25.6 Hz, C-4); 106.6 (CH, d, $J_{F.C}$ = 23.6 Hz, C-6); 27.6 (CH_3, C-2') ppm.

1-(5-Chloro-1H-indol-3-yl)ethanone (3.6):

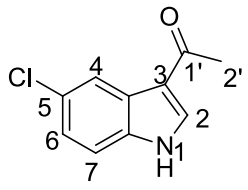

Yield = 48%; **^{1}H NMR (DMSO, 300 MHz)**: δ_H 12.13 (s, 1H, NH-1); 8.39 (s, 1H, H-2); 8.15 – 8.14 (d, 1H, J = 2.1 Hz, H-4); 7.50 - 7.47 (d, 1H, J = 8.8 Hz, H-7); 7.24 – 7.21 (dd, 1H, J_1 = 8.6 Hz , J_2 = 2.1 Hz, H-6); 2.44 (s, 3H, H-2') ppm; **^{13}C NMR (DMSO, 75**

MHz)): δ_C 193.2 (q_c, C-1'); 136.3 (q_c, C-2); 135.6 (CH, C-7a); 126.8 (q_c, C- 3a); 124.1 (q_c, C-5); 123.2 (CH, C-6); 120.8 (CH, C-4); 116.8 (q_c, C-7); 114.2 (CH, C-3); 27.6 (CH_3, C-2') ppm.

4.1.3 General procedure for the synthesis of N-modified 3-acetylindole 3.7:

To a stirred solution of 1-(1-benzyl-5-chloro-1H-indol-3-yl)ethanone (1 e.q) in DMF (4 mL) at 0 °C was added NaH. After 15 min, benzyl bromide (0.9 mL) was added dropwise and allowed to react for 1 h after which time the reaction was quenched with sat. $NaHCO_3$. The reaction was extracted with EtOAc (15 mL) and concentrated *in vacuo* followed by purification *via* normal phase flash chromatography (80% CH_2Cl_2: 20 % EtOAc). *In vacuo* solvent removal afforded a brown tarry solid which was stored for the next synthetic step.

1-(1-Benzyl-5-chloro-1H-indol-3-yl)ethanone (3.7):

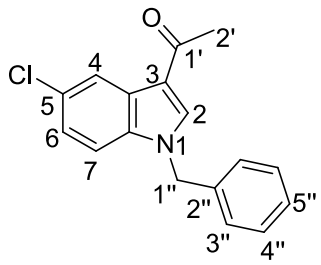

Yield = 95%; **^{1}H NMR (DMSO, 400 MHz)**: δ_H 8.6 (s, 1H, H-2); 8.17 – 8.16 (d, 1H, *J* = 2.1 Hz, H-4); 7.58 – 7.56 (d, 1H, *J* = 8.8 Hz, H-7); 7.35 – 7.27 (m, 6H, H-6, H-3'', H-4'', H-5''); 5.51(s, 2H, H-1''); 2.46 (s, 3H, H - 2') ppm; **^{13}C NMR (DMSO, 100 MHz))**: δ_C 192.9 (q_c, C-1'); 139.3 (q_c, C-2); 137.2 (q_c, C-2'') 135.5 (CH, C-7a); 129.2 (q_c, C-4''); 128.3 (q_c, C-3a); 127.7 (CH, C-3'') 127.5 (q_c, C-3a); 127.4 (CH, C-5); 123.4 (q_c, C-5); 121.1 (CH, C-6); 116.1 (q_c, C-3); 113.3 (CH, C-7); 50.3 (CH_2, C-1'') 27.6 (CH_3, C-2') ppm.

4.1.4 General procedure for the synthesis of 2-bromo-1-(1*H*-indol- 3-yl)ethanones 3.8 – 3.10:

A solution of 3-acetylindole (3.14 mmol, 1 eq.) in $CHCl_3$ (98 mL) was added to a vigorously stirred suspension of $CuBr_2$ (1.262 g, 5.65 mmol, 1.8 eq.) in EtOAc (74 mL) and heated to reflux, with constant monitoring by TLC. After 6 h, the reaction mixture was allowed to cool, washed with water (2 × 20 mL), sat. brine (2 × 20 mL) and dried over anhydrous $MgSO_4$. Solvent was removed *in vacuo* followed by purification *via* normal flash chromatography (100% CH_2Cl_2). *In vacuo* solvent removal afforded a white cystalline solid which was dissolved in cold acetone and allowed to evaporate slowly.

2-Bromo-1-(5-fluoro-1*H*-indol-3-yl)ethanone (3.8):

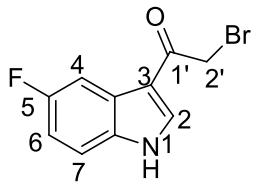

Yield = 33.5%. **^{1}H NMR (DMSO, 300 MHz)**: δ_H 12.44 (s, 1H, NH-1); 8.54 (d, 1H, J = 3.31 Hz, H-2); 7.83 – 7.79 (dd, 1H, H-4, J_1 = 9.9 Hz , J_2 = 2.5 Hz); 7.54 – 7.49 (m, 1H, H-7); 7.14 – 7.07 (m, 1H, H-6); 4.65 (s, 2H, H-2”); **^{13}C NMR (DMSO, 75 - MHz)** : δ_C 186.9 (q_c, C-1’); 157.6 (q_c, C-5); 137.2 (CH, C-2); 133.8 (q_c, C-7a); 126.5 (d, q_c, C-3a); 114.1 (q_c, d, $J_{F.C}$ = 4.4 Hz, C-3); 113.9 (CH, d, $J_{F.C}$ = 10.5 Hz, C-6); 111.7 (CH, d, $J_{F.C}$ = 25.3 Hz, C-4) 106.4 (CH, C-7); 33.9 (CH_2, C-2’) ppm.

2-Bromo-1-(1*H*-indol3-yl)ethanone (3.9):

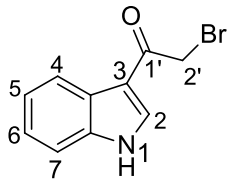

Yield = 51.6%; **^{1}H NMR (DMSO, 300MHz)**: δ_H 11.97 (s, 1H, NH-1); 8.29 (1H, d, *J* = 3.16 Hz, H-2); 8.18 (1H, d, *J* = 11.13 Hz, H-4); 7.46 (1H, m, H-7); 7.15 - 7.11 (2H, m, H-5, H-6); 4.40 (2H, s, H-2') ppm; **^{13}C NMR (DMSO, 75- MHz)** : δ_C 186.9 (q_c, C–1'); 137.2 (q_c, C-7a); 135.8 (CH, C-2); 125.9 (q_c, C-3a); 123.7 (CH, C-4); 122.7 (CH, C-6); 121.7 (CH, C-5); 113.9 (q_c, C-3); 112.8 (CH, C-7); 34.0 (CH_2, C-2') ppm

2-bromo-1-(5-chloro-1H-indol-3-yl)ethanone (3.10):

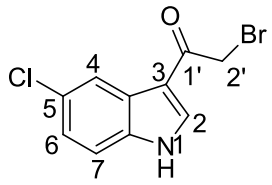

Yield = 35.6% **^{1}H NMR (Acetone, 300 MHz)**: δ_H 11.36 (s, 1H, NH - 1); 8.46 – 8.45 (d, 1H, *J* = 3.6 Hz, H-2); 8.30 – 8.29 (d, 1H, *J* = 2.1 Hz, H-4); 7.58 – 7.55 (dd, 1H, J_1 = 0.5 Hz, J_2 = 8.6 Hz, H-6); 7.28 – 7.25 (dd, 1H, J_1 = 2.2 Hz, J_2 = 8.7 Hz, H-7); 4.54 (s, 2H, H-2'); **^{13}C NMR (Acetone, 75 MHz)**: δ_C 186.9 (q_c, C-1'); 136.9 (q_c, C-7a); 135.7 (CH, C-2); 127.4 (q_c, C-3a); 124.1 (q_c, C-5); 123.8 (CH, C-6); 120.7 (CH, C-4); 114.5 (q_c, C-3); 113.6 (CH, C-7); 31.1 (CH, C-2') ppm.

4.1.5 General procedure for the synthesis of α-brominated N-modified 3-acetylindole 3.11:

A solution of 1-(1-benzyl-5-chloro-1H-indol-3-yl)-2-bromoethanone (0.176 mmol, 1 eq.) in CHCl3 (5.5 mL) was added to a vigorously stirred suspension of $CuBr_2$ (70 mg, 0.317 mmol, 1.8 eq.) in EtOAc (4 mL) and heated to reflux, with constant monitoring by TLC. After 2 h, the reaction mixture was allowed to cool, washed with water (2 × 20 mL), sat. brine (2 × 20 mL) and dried over anhydrous $MgSO_4$. Solvent was removed *in vacuo* followed by purification *via* normal phase flash chromatography (80% CH_2Cl_2: 20% EtOAc). *In vacuo* solvent removal afforded a beige solid which was dissolved in cold acetone and allowed to evaporate slowly.

1-(1-Benzyl-5-chloro-1H-indol-3-yl)-2-bromoethanone (3.11):

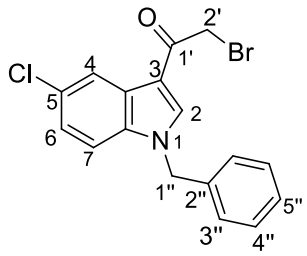

Yield = 92 % **^{1}H NMR (DMSO, 400 MHz)**: δ_H 8.78 (s, 1H, H - 2); 8.15 – 8.14 (d, 1H, *J* = 2.1 Hz, H - 4); 7.65 - 7.63 (d, 1H, *J* = 8.7 Hz, H - 7); 7.24 - 7.20 (dd, 1H, J_1 = 8.7 Hz, J_2 = 2.1 Hz, H - 6); 2.44 (s, 3H, H - 2') ppm;

4.1.6 Procedure for the synthesis of methyl 4-phenoxybenzoate 3.12:

Thionyl chloride was added to 4-phenoxybenzoic acid (2.33 mmol). The mixture was allowed to reflux under nitrogen at 70 ^{o}C and after 2 h sodium methoxide was added and the fumes allowed to escape. An extraction with EtOAc was done and the organic phase washed with sat. brine. *In vacuo* solvent removal was followed by purification *via* normal phase flash chromatography (80% Hexane: 20% EtOAC). The resultant brown solid which was collected after *in vacuo* solvent removal was dissolved in cold acetone and allowed to evaporate slowly.

Methyl 4-phenoxybenzoate (3.12):

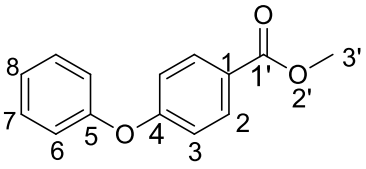

Yield = 40.2% **^{1}H NMR (DMSO, 300MHz)**: δ_H 7.985 – 7.95 (d, 2H, *J* = 8.8 Hz, H-2); 7.49 – 7.42 (t, 2H, H-7); 7.27 – 7.22 (t, 1H, H-8); 7.14 – 7.12 (d, 2H, *J* = 8.6 Hz, H-6) 7.06 – 7.03 (dd, 2H, J_1 = 2.1 Hz, J_2 = 8.9 Hz, H-3); 3.82 (s, 3H, H - 2'); **^{13}C NMR (DMSO, 75 MHz)**: δ_C 166.6 (q_c, C-1'); 161.8 (q_c, C-4); 155.3 (q_c, C-5); 132.0 (CH, C-2); 130.8 (CH, C-7); 125.3 (q_c, C-1); 124.4 (CH, C-8); 120.6 (CH, C-6); 117.7 (CH, C-3); 52.5 (CH_3, C-2') ppm.

4.1.7 Procedure for the synthesis of methyl 4-mercaptobenzoate 3.14:

Thionyl chloride was added to 4-mercaptobenzoic acid (4.094 mmol). The mixture was allowed to reflux under nitrogen at 70 ^{o}C and after 2 h sodium methoxide was added and the fumes vented. Organics were extracted with EtOAc and washed with

sat. brine. *In vacuo* solvent removal afforded a beige solid which was dissolved in cold acetone and allowed to evaporate slowly and stored for the final synthetic step.

Methyl 4-mercaptobenzoate (3.14):

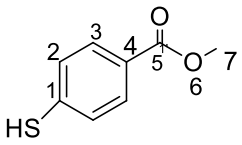

Yield = 43.2% **^{1}H NMR (DMSO, 300MHz)**: δ_H 7.96 – 7.93 (d, 2H, *J* = 8.5 Hz, H-3); 7.67 – 7.64 (d, 2H, *J* = 8.5 Hz, H-2); 3.85 – 3.83 (d, 3H, *J* = 6.2 Hz, H-2') ppm; **^{13}C NMR (DMSO, 75 MHz)**: δ_C 165.5 (q_c, C-1'); 141.2 (q_c, C-1); 130.3 (CH, C-3); 128.4 (CH, C-2); 126.3 (q_c, C-4); 39.2 (CH_3, C-2') ppm.

4.1.8 Procedure for the synthesis of 4-mercaptobenzonitrile 3.16:

To a stirred suspension of 4-mercaptobenzamide (3.55 mmol, 1 eq.) in DMF was added $POCl_3$ (8.88 mmol, 2.5 eq.) at 0 ^{o}C. The mixture was allowed to react for 2 h and then extracted with EtOAc and the organic phase washed with sat. brine. *In vacuo* solvent removal afforded a yellow liquid which when left to stand became a yellow solid, which was stored for the final step of the synthetic pathway.

4-Mercaptobenzonitrile (3.16):

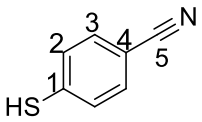

Yield = 93.5% **^{1}H NMR (DMSO, 300MHz)**: δ_H 7.85 – 7.78 (d, 2H, *J* = 8.7 Hz, H-3); 7.73 – 7.69 (d, 2H, *J* = 7.6 Hz, H-2) ppm; **^{13}C NMR (DMSO, 75 MHz)**: δ_C 141.9 (q_c C-4); 133.7 (q_c C-1); 129.7 (CH, C-3); 127.0 (CH, C-2); 118.8 (q_c C-5) ppm.

4.1.9 General procedure for the synthesis of nucleophilic coupling reaction to generate α-aryl substituted 3-indolylethanones 3.17 – 3.27:

To a stirred suspension of 2- bromo-1-(1*H*-indol-3-yl)ethanone (1 eq.) and K_2CO_3 (2 eq.) in acetone was added a relevant nucleophile (2 eq.). The reaction mixture was heated to reflux and after 5 h was cooled and extracted with EtOAc. The organic phase was washed with water and sat. brine. Crude organic mixtures were purified by normal phase flash chromatography (80% Hexane: 20% EtOAC). *In vacuo* solvent removal resulted in white crystals. These resultant crystals were washed with cold chloroform to further purify and yield the desired product.

2-(4-Bromophenylthio)-1-(5-fluoro-1*H*-indol-3-yl)ethanone (3.17):

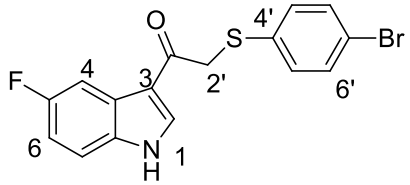

White crystalline solid (62.9%); m.p: 177 – 179 °C, **^{1}H NMR (DMSO, 600 MHz)**: δ_H 12.19 (s, 1H, NH-1); 8.56 (s, 1H, H-2); 7.81 – 7.79 (dd, 1H ,J_1= 9.8 Hz, J_2 = 2.7 Hz, H-4); 7.51 – 7.46 (m, 3H, H-7, H-5'); 7.34 – 7.32 (m, 2H, H-5'); 7.10 – 7.07 (t, 1H, *J* = 9.2 Hz, H-6); 4.48 (s, 2H, C-2') ppm; **^{13}C NMR (DMSO, 150 MHz)**: δ_C 188.8 (q_c, C-1'); 159.5 – 157.9 (q_c, d, $J_{F.C}$ = 235.4 Hz, C-5); 136.4 (CH, C-2) 136.0 (CH, C-4'); 133.2

(q_c, C-7a); 131.6 (CH, C-6'); 129.8 (CH, C-5'); 126.1 – 126.0 (q_c, d, $J_{F.C}$ = 11.1 Hz, C-3a); 118.5 (q_c, C-7'); 115.0 – 114.9 (q_c, d, $J_{F.C}$ = 4.3 Hz, C-3); 113.6 – 113.5 (CH, d, $J_{F.C}$ = 9.7 Hz, C-7); 111.3 – 111.1 (CH, d, $J_{F.C}$ = 25.8 Hz, C-6); 106.1 – 105.9 (CH, d, $J_{F.C}$ = 24.3 Hz, C-4); 39.8 (CH_2, C-2') ppm; IR (film) V_{max} cm^{-1} 3197.3, 2921.9, 1714.8, 1612.2, 1467.4, 1430.9, 1168.9, 810.9, 706.7; HRESMS *m/z* 363.9779 (calcd for $C_{16}H_{12}NOS^{79}BrF$ $[M+H]^+$ 363.9807).

1-(5-Fluoro-1*H*-indol-3-yl)-2-(4-nitrophenylthio)ethanone (3.18):

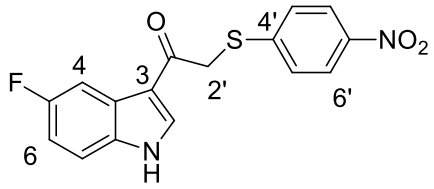

White crystalline solid (54.6%); m.p: 210 – 212 °C, **^{1}H NMR (DMSO, 600MHz)**: δ_H 12.25 (s, 1H, NH-1); 8.70 – 8.65 (d, 1H, *J* = 3.3 Hz, H-2); 8.14 – 8.13 (m, 2H, H-6'); 7.81 – 7.79 (d, 1H, *J* = 8.2 Hz, H-4); 7.57 – 7.59 (d, 2H, *J* = 8.8 Hz, H-5'); 7.53 – 7.51 (m, 1H, H-7); 7.12 – 7.08 (t, 1H, *J* = 9.3 Hz, H-6); 4.73 (s, 2H, H- 2') ppm; **^{13}C NMR (DMSO, 150 MHz)**: δ_C 187.9 (q_c, C-1'); 159.5 – 157.9 (q_c, d, $J_{F.C}$ = 235.6 Hz, C-5) 147.4 (CH, C-4'); 144.4 (q_c, C-7'); 136.6 (CH, C-2); 133.2 (q_c, C-7a); 126.4 (CH, C-5') 126.0 (q_c, C-3a); 125.9 (CH, C-5'); 123.8 (CH, C-6'); 114.9 – 114.8 (CH, d, $J_{F.C}$ = 9.96 Hz, C-7); 113.7 – 113.6 (q_c, d, J_{FC} = 4.5 Hz, C-3); 111.4 – 111.2 (CH, d, $J_{F.C}$ = 26.2 Hz, C-6); 106.1 – 105.9 (CH, d, $J_{F.C}$ = 24.9 Hz, C-4); 38.7 (CH_2, C-2') ppm; IR (film) V_{max} cm^{-1} 3103.5, 2917.7, 2850.5, 1727.6, 1613.1, 1505.8, 1174.2, 840.2, 737.9; HRESMS *m/z* 331.0533 (calcd for $C_{16}H_{12}N_2O_3SF$ $[M+H]^+$ 331.0553).

Methyl 4-(2-(1H-indol-3-yl)-2-oxoethylthio)benzoate (3.19):

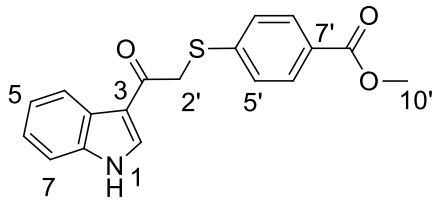

White crystalline solid (25.7%); m.p: 99 – 101 °C, **^{1}H NMR (DMSO, 600 MHz)**: δ_H 12.11 (s, 1H, NH-1); 8.54 – 8.53 (d, 1H, *J* = 3.2 Hz, H-2); 8.14 – 8.12 (d, 1H, *J* = 8.1 Hz, H-4); 7.85 – 7.84 (d, 2H, *J* = 8.6 Hz, H-6'); 7.50 – 7.46 (m, 3H, H-5', H-7); 7.24 – 7.18 (m, 2H, H-5, H-6); 4.61 (s, 2H, H-2'); 3.81 (s, 3H, H-10') ppm; **^{13}C NMR (DMSO, 150 MHz)**: δ_C 188.4 (q_c, C-1'); 165.9 (q_c, C-8'); 144.0 (q_c, C-4'); 136.6 (q_c, C-7a); 135.1 (CH, C-2); 129.5 (CH, C-6'); 126.3 (CH, C-5'); 125.9 (q_c, C-7'); 125.4 (q_c, C-3a); 123.1 (CH, C-4); 122.1 (CH, C-6); 121.2 (CH, C-5); 114.9 (q_c, C-3); 112.3 (CH, C-7); 52.0 (CH_3, C-10'); 39.2 (CH_2, C-2') ppm. IR (film) V_{max} cm^{-1} 3261.2, 2920.7, 2850.8, 1713.6, 1518.2, 1432, 1274.7 1109.1; HRESMS *m/z* 326.0842 (calcd for $C_{18}H_{16}NO_3S$ $[M+H]^+$ 326.0851)

1-(1*H*-Indol-3-yl)-2-(4-nitrophenoxy)ethanone (3.20):

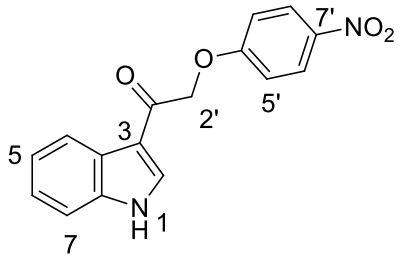

White crystalline solid (66.3 %); m.p: 220 – 222 °C, **^{1}H NMR (DMSO, 600 MHz)**: δ_H 8.52 (s, 1H, H-2); 8.24 – 8.18 (dd, 2H, J_1= 7.0 Hz, J_2 = 2.2 Hz, H-6); 8.14 – 8.11

(dd, 1H, J_1= 7.0 Hz, J_2 = 2.1 Hz, H-4); 7.53 – 7.50 (dd, 1H, J_1 = 7.0 Hz, J_2 = 1.8 Hz, H-7); 7.27 – 7.19 (m, 2H, H-5'); 7.18 – 7.15 (dd, 2H, J_1 = 7.0 Hz, `J_2 = 2.2 Hz, H-5, H-6); 5.55 (s, 2H, H-2'). **^{13}C NMR (DMSO, 150 MHz))**: δ_C 188.3 (q_c, C-1'); 163.8 (q_c, C-4'); 141.0 (q_c, C-7'); 136.5 (q_c, C-7a); 134.3 (CH, C-2); 125.9 (CH, C-6'); 125.4 (q_c, C-3a); 123.3 (CH, C-6); 122.2 (CH, C-4); 121.2 (CH, C-5); 115.3 (CH, C-5'); 113.1 (q_c, C-3); 112.4 (CH, C-7); 70.3 (CH_2, C-2') ppm; IR (film) V_{max} cm^{-1} 3172.1, 2922.2, 1727.9, 1635.6, 1505, 1428.7, 1235.3, 1111.8; HRESMS *m/z* 297.0871 (calcd for $C_{16}H_{13}N_2O_4$ $[M+H]^+$ 297.0875).

4-(2-(1H-Indol-3-yl)-2-oxoethylthio)benzonitrile (3.21):

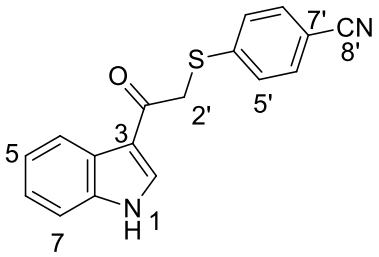

Brown crystalline solid (22.3%); m.p: 204 – 206 °C, **^{1}H NMR (DMSO, 300 MHz)**: δ_H 11.25 (s, 1H, NH-1); 8.50 – 8.49 (d, 1H, J = 3.1 Hz, H-2); 8.29 – 8.28 (m, 1H, H-4); 7.67 – 7.65 (dd, 2H, J_1 = 6.6, J_2 = 2.0 Hz, H-5'); 7.58 – 7.56 (dd, 2H, J_1 = 6.61 Hz, J_2 = 2.25 Hz, H-6'); 7.54 – 7.53 (m, 1H, H-7); 7.22 – 7.27 (m, 2H, H-5, H-6); 4.61 (s, 2H, H-2'); **^{13}C NMR (DMSO, 75 MHz))**: δ_C 187.8 (q_c, C-1'); 144.8 (CH, C-4'); 136.8 (CH, C-7'); 133.7 (q_c, C-7a); 132.0 (CH, C-2'); 126.8 (CH, C-6'); 125.8 (CH, C-5'); 123.2 (q_c, C-3a); 122.0 (CH, C-4); 121.7 (CH, C-6); 118.4 (q_c, C-8'); 115.4 (CH, C-5); 111.8 (q_c, C-3); 107.8 (CH, C-7); 38.9 (CH_2, C-2') ppm; IR (film) V_{max} cm^{-1} 3211.5, 2947.5,

2220.3, 1627.8, 1402, 1239, 1137.6, 1088.6; HRESMS *m/z* 293.0739 (calcd for $C_{17}H_{13}N_2OS$ $[M+H]^+$ 293.0749)

1-(1-benzyl-5-chloro-1H-indol-3-yl)-2-(4-nitrophenylthio)ethanone (3.22):

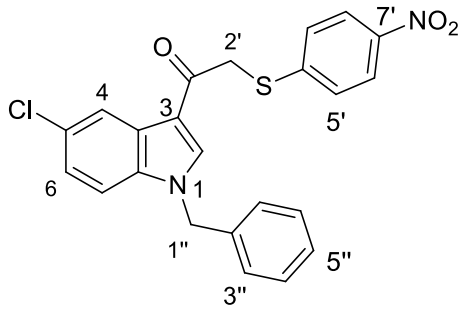

Yellow crystalline solid (20.2%); m.p: 155 – 157 °C, **^{1}H NMR (DMSO, 400 MHz)**: δ_H 8.87 (s, 1H, H-2); 8.12 – 8.14 (m, 3H, H-4, H-6'); 7.58 – 7.65 (m, 3H, H-7, H-5'); 7.27 – 7.36 (m, 6H, H-6, H-3", H-4", H-5"); 5.55 (s, 2H, H-1"); 4.74 (s, 2H, H-2') ppm; **^{13}C NMR (DMSO, 100 MHz))**: δ_C 187.9 (q_c, C-1'); 147.2 (q_c, C-7'); 144.5 (q_c, C-4'); 139.3 (q_c, C-2"); 136.6 (CH, C-2); 135.1 (q_c, C-7a); 128.8 (q_c, C-3a); 127.9 (CH, C-3"); 127.4 (CH, C-5'); 127.3 (CH, C-5"); 127.1 (q_c, C-5); 126.5 (CH, C-4''); 123.8 (CH, C-6'); 123.4 (CH, C-6); 120.6 (CH, C-4); 113.7 (q_c, C-3); 113.1 (CH, C-7); 50.6 (CH_2, C-1"); 39.3 (CH_2, C-2') ppm; IR (film) V_{max} cm^{-1} 3111.9, 2919.3, 2850.2, 1950.9, 1710.6, 1643.8, 1393, 1182.1; HRESMS *m/z* 437.0732 (calcd for $C_{23}H_{17}N_2O_3S^{35}Cl$ $[M+H]^+$ 437.0738).

2-(1H-Benzo[d]imidazol-2-ylthio)-1-(1H-indol-3-yl)ethanone (3.23):

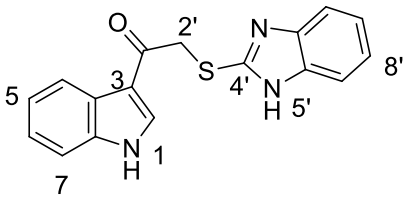

Transparent crystalline solid (73.8 %); m.p: 205 – 207 °C, **^{1}H NMR (DMSO, 300 MHz)**: δ_H 12.65 (s, 1H, NH-1); 12.13 (s, 1H, NH-5); 8.52 – 8.51 (d, 1H, *J* = 3.2 Hz, H-2); 8.13 – 8.11 (d, 1H, *J* = 7.0 Hz, H-4); 7.51 – 7.48 (m, 1H, H-7); 7.45 – 7.38 (m, 2H, H-7'); 7.26 – 7.16 (m, 2H, H-8'); 7.13 – 7.09 (m, 2H, H-5, H-6); 4.85 (s, 2H, H-2'); **^{13}C NMR (DMSO, 75 MHz))**: δ_C 188.5 (q_c, C-1'); 150.4 (q_c, C-4'); 143.9 (q_c, C-6'); 137.0 (q_c, C-7a); 135.4 (CH, C-2); 125.8 (q_c, C-3a); 123.6 (CH, C-8'); 122.6 (CH, C-4); 121.6 (CH, C-6); 117.6 (CH, C-5); 115.2 (q_c, C-3); 112.8 (CH, C-7'); 110.9 (CH, C-7); 39.6 (CH_2, C-2') ppm; IR (film) V_{max} cm^{-1} 3171.6, 2221.8, 1605.7, 1506.6, 1429.3, 1300.6, 1156.2; HRESMS *m/z* 308.0850 (calcd for $C_{17}H_{14}N_3OS$ $[M+H]^+$ 308.0858)

1-(1H-Indol-3-yl)-2-(5-nitropyridin-2-yloxy)ethanone (3.24):

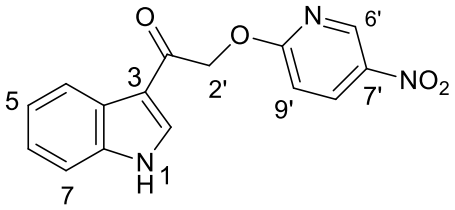

White crystalline solid (12.7%); m.p: 258 – 260 °C, **^{1}H NMR (DMSO, 300 MHz)**: δ_H 12.19 (s, 1H, NH-1); 9.23 – 9.22 (d, 1H, *J* = 3.1 Hz, H-8'); 8.61 (s, 1H, H-2); 8.24 – 8.20 (dd, 1H, J_1 = 3.1 Hz, J_2 = 10.0 Hz, H-4); 8.11 – 8.08 (dd, 1H, J_1= 7.1 Hz, J_2 = 2.1 Hz, H-6'); 7.54 – 7.51 (d, 1H, J_1 = 8.0 Hz, J_2 = 1.9 Hz, H-7); 7.28 – 7.19 (m, 2H, H-5, H-6); 6.57 – 6.54 (d, 1H, *J* = 10.0 Hz, H-9'); 5.52 (s, 2H, H-2'); **^{13}C NMR (DMSO, 75**

MHz)): δ_C 186.3 (q_c, C-1'); 160.9 (q_c, C-4'); 143.1 (CH, C-6'); 136.6(q_c, C-7'); 134.6 (q_c, C-7a); 133.9 (CH, C-8'); 129.8 (CH, C-2); 125.3 (q_c, C-3a); 123.3 (CH, C-4); 122.3 (CH, C-6); 121.0 (CH, C-5); 118.1 (q_c, C-3); 113.5 (CH, C-7); 112.5 (CH, C-9'); 55.2 (CH_2, C-2') ppm; IR (film) V_{max} cm^{-1} 3403.7, 3126.8, 1693.4, 1602.6, 1458.1, 1280, 1167.7, 1108.6; HRESMS *m/z* 298.0824 (calcd for $C_{15}H_{12}N_3O_4$ $[M+H]^+$ 298.0828)

4-(2-(1H-Indol-3-yl)-2-oxoethoxy)benzonitrile (3.25):

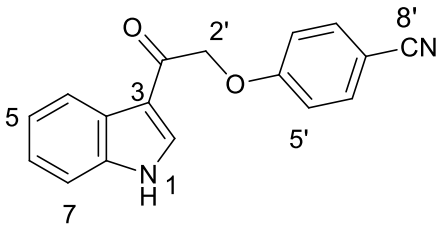

White crystalline solid (75.6 %); m.p: 237 – 239 °C, **^{1}H NMR (DMSO, 300 MHz)**: δ_H 12.12 (s, 1H, NH-1); 8.51 (s, 1H, H-2); 8.14 – 8.12 (d, 1H, *J* = 3.0 Hz, H-4); 7.79 – 7.75 (d, 2H, *J* = 7.8 Hz, H-6'); 7.52 – 7.50 (d, 1H, *J* = 7.9 Hz, H-7); 7.26 – 7.18 (m, 2H, H-5'); 7.15 – 7.12 (d, 2H, *J* = 8.8 Hz, H-5, H-6); 5.47 (s, 2H, H-2'); **^{13}C NMR (DMSO, 75 MHz))**: δ_C 188.5 (q_c C-1'); 161.9 (q_c, C-4'); 136.4 (q_c, C-7a); 134.2 (overlapping CH, C-2 and CH, C-6'); 125.3 (q_c, C-3a); 123.2 (CH, C-4); 122.1 (CH, C-6); 121.2 (CH, C-5); 119.2 (q_c, C-8'); 115.8 (CH, C-5'); 113.2 (q_c, C-3); 112.3 (q_c, C-7); 102.9 (q_c, C-7'); 66.9 (CH_2, C-2') ppm; IR (film) V_{max} cm^{-1} 3236.2, 3054.5, 2919.4, 2851.9, 1711.3, 1626.7, 1500.6, 1409.3, 1245.1, 1153.7; HRESMS *m/z* 277.0968 (calcd for $C_{17}H_{13}N_2O_2$ $[M+H]^+$ 277.0977).

4-(2-(5-Chloro-1H-indol-3-yl)-2-oxoethoxy)benzonitrile (3.26):

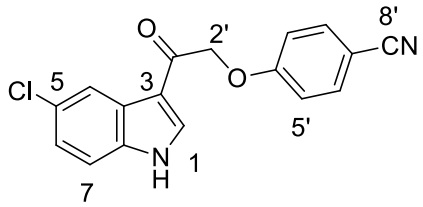

White crystalline solid (35.8 %); m.p: 229 – 231 °C, **^{1}H NMR (DMSO, 300 MHz)**: δ_H 12.32 (s, 1H, NH-1); 8.57 (s, 1H, H-2); 8.11 – 8.10 (d, 1H, *J* = 2.0 Hz, H-4); 7.78 – 7.76 (d, 2H, *J* = 8.9 Hz, H-6'); 7.55 – 7.53 (d, 1H, *J* = 8.7 Hz, H-7); 7.28 – 7.26 (dd, 1H, J_1 = 8.7 Hz, J_2 = 2.0 Hz, H-6); 7.15 – 7.13 (d, 2H, *J* = 8.9 Hz, H-5'); 5.47 (s, 2H, H-2'); **^{13}C NMR (DMSO, 75 MHz))**: δ_C 188.7 (q_c C-1'); 161.8 (q_c C-4'); 135.5 (q_c C-7a); 134 .9 (CH, C-2); 134.2 (CH, C-6'); 126.9 (q_c, C-3a); 126.5 (q_c, C-5); 123.3 (CH, C-6); 120.3 (CH, C-4); 119.2 (q_c, C-8'); 115.8 (CH, C-5'); 114.1 (q_c, C-3); 112.8 (CH, C-7); 103.1 (q_c, C-7'); 66.9 (CH_2, C-2') ppm; IR (film) V_{max} cm^{-1} 3177.8, 2917.8, 2224.5, 1659.9, 1509.3, 1250.9, 1153.8; HRESMS *m/z* 311.0591 (calcd for $C_{17}H_{12}N_2O_2{}^{35}Cl$ $[M+H]^+$ 311.0587).

4-(2-(5-chloro-1H-indol-3-yl)-2-oxoethylthio)benzonitrile (2.27):

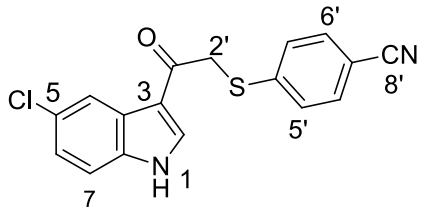

White crystalline solid (35.8 %); m.p: 249 – 251 °C, **^{1}H NMR (DMSO, 300 MHz)**: δ_H 12.33 (s, 1H, NH-1); 8.64 – 8.63 (d, 1H, *J* = 2.7 Hz, H-2); 8.10 – 8.09 (d, 1H, *J* = 2.1 Hz, H-4); 7.73 – 7.71 (d, 2H, *J* = 8.5 Hz, H-6'); 7.54 – 7.52 (t, 3H, *J* = 8.9 Hz, H-5', H-7); 7.25 – 7.27 (dd, 1H, J_1 = 8.7 Hz, J_2 = 2.1 Hz, H-6); 4.66 (s, 2H, H-2'); **^{13}C NMR (DMSO, 75 MHz))**: δ_C 188.5 (q_c, C-1'); 144.5 (q_c, C-4'); 136.5 (q_c, C-7'); 135.2 (q_c, C-7a); 132.4 (overlapping CH, C-2 and CH, C-6'); 126.9 (CH, C-5'); 126.7 (q_c, C-3a); 126.6 (q_c, C-5); 120.4 (CH, C-4); 119.0 (q_c, C-8'); 114.5 (q_c, C-3); 114.1 (q_c, C-6); 107.1 (q_c, C-7); 39.8 (CH_2, C-2') ppm; IR (film) V_{max} cm^{-1} 3203.6, 2907.3, 2219, 1634, 1592.6, 1402.8, 1229.3, 1142.2; HRESMS *m/z* 438.9414 (calcd for $C_{17}H_{12}N_2OS^{35}Cl$ $[M+H]^+$ 438.9416)**.**

4.2 Growth inhibition assays

4.2.1 *Plasmodium falciparum* growth inhibition assay

Malaria parasites (*Plasmodium falciparum* strain 3D7) are maintained in RPMI 1640 medium containing 2 mM L-glutamine and 25 mM Hepes (Lonza). The medium is further supplemented with 5% Albumax II, 20 mM glucose, 0.65 mM hypoxanthine, 60 µg/mL gentamycin and 2 – 4% hematocrit human red blood cells. The parasites are cultured at 37 °C under an atmosphere of 5% CO_2, 5% O_2, 90% N_2 in sealed T25 or T75 culture flasks.

For screening compounds against malaria parasites, compounds at 20 µM or 25 µg/ml (natural extracts) are added to parasite cultures in 96-well plates and incubated for 48 h in a 37 °C CO_2 incubator. After 48 h the plates are removed from the incubator. Twenty µL of culture is removed from each well and mixed with 125 µL

of a mixture of Malstat solution and NBT/PES solution in a fresh 96-well plate. These solutions measure the activity of the parasite lactate dehydrogenase (pLDH) enzyme in the cultures. A purple product is formed when pLDH is present, and this product can be quantified in a 96-well plate reader by absorbance at 620 nm (Abs620). The Abs620 reading in each well is thus an indication of the pLDH activity in that well and also the number of parasites in that well.

For each compound concentration, % parasite viability – the pLDH activity in compound-treated wells relative to untreated controls – is calculated. Compounds are usually tested in duplicate wells, and a standard deviation (SD) is derived. For comparative purposes, Chloroquine (an anti-malarial drug) is used as a drug standard and yields IC_{50} values in the range 0.01 – 0.05 µM. These experiments were conducted by Michelle Isaacs.

4.2.2 HeLa cell growth inhibition assay

To assess the IC_{50} value for cytotoxicity of the compounds, they are incubated at a range of concentrations from 250 µM down in a 3-fold dilution series in 96-well plates containing HeLa cells for 48 h. The numbers of cells surviving drug exposure are determined by using the resazurin based reagent and reading resorufin fluorescence in a multiwell plate reader.

For each compound concentration, % cell viability – the resorufin fluorescence in compound-treated wells relative to untreated controls – is calculated. Compounds are usually tested in duplicate wells, and a standard deviation (SD) is derived. For each compound, percentage viability is then plotted against Log (compound concentration) and the IC_{50} (50% inhibitory concentration) obtained from the resulting

dose-response curve by non-linear regression. For comparative purposes, Emetine (which induces cell apoptosis) is used as a drug standard and yields IC_{50} values in the range 0.1 – 0.05 µM. These experiments were conducted by Michelle Isaacs.

References

(1) WHO. WHO | Malaria http://www.who.int/mediacentre/factsheets/fs094/en/ (accessed Jul 5, 2017).

(2) CDC - Malaria https://www.cdc.gov/malaria/ (accessed Jul 5, 2017).

(3) Marquet, S. *Infect. Genet. Evol.* **2017**, doi.org/10.1016/j.meegid.2017.06.001.

(4) WHO. *World Malaria Report 2015*; Geneva, 2015.

(5) RBM. What is Malaria http://www.rollbackmalaria.org/about-malaria/what-is-malaria (accessed Aug 10, 2017).

(6) Rijken, M. J.; Charlotte de Wit, M.; Mulder, E. J.; Kiricharoen, S.; Karunkonkowit, N.; Paw, T.; Visser, G. H.; McGready, R.; Nosten, F. H.; Pistorius, L. R. *Malar. J.* **2012**, *11* (222).

(7) Rijken, M. J.; Papageorghiou, A. T.; Thiptharakun, S.; Kiricharoen, S.; Dwell, S. L. M.; Wiladphaingern, J.; Pimanpanarak, M.; Kennedy, S. H.; Nosten, F.; McGready, R. *PLoS One* **2012**, *7* (2), e31411.

(8) Dorman, E. K.; Shulman, C. E.; Kingdom, J.; Bulmer, J. N.; Mwendwa, J.; Peshu, N.; Marsh, K. *Ultrasound Obstet. Gynecol.* **2002**, *19* (2), 165–170.

(9) Uneke, C. J. *Yale J. Biol. Med.* **2007**, *80*, 39–50.

(10) Drewry, Martin; Betts, A. S. N. Key Facts: Malaria https://www.healthpovertyaction.org/info-and-resources/the-cycle-of-poverty-and-poor-health/infectious-diseases/malaria/key-facts/ (accessed Aug 10, 2017).

(11) Red Cross EU. Economic Cost of Malaria on Countries http://www.malariaconsortium.org/userfiles/file/Past events/factsheet2 - malaria and poverty.pdf (accessed Aug 10, 2017).

(12) Gallup, J. L.; Sachs, J. D. *Am. J. Trop. Med. Hyg.* **2001**, *64* (1), https://www.ncbi.nlm.nih.gov/books/NBK2624/ (accessed Aug 10 2017)

(13) Bloomberg, J. H. Malaria Free Future https://www.malariafreefuture.org/malaria (accessed Aug 10, 2017).

(14) Raghavendra, K.; Barik, T. K.; Reddy, B. P. N.; Sharma, P.; Dash, A. P. *Parasitol. Res.* **2011**, *108* (4), 757–779.

(15) PATH. Life cycle of the malaria parasite | Malaria Vaccine Initiative http://www.malariavaccine.org/malaria-and-vaccines/vaccine-development/life-cycle-malaria-parasite (accessed Oct 3, 2017).

(16) Flannery, E. L.; Chatterjee, A. K.; Winzeler, E. A. *Nat Rev Microbiol* **2013**, *11* (12), 849–862.

(17) MMV. Parasite lifecycle https://www.mmv.org/malaria-medicines/parasite-lifecycle (accessed Oct 4, 2017).

(18) Carvalho, L. J. M.; Daniel-Ribeiro, C. T.; Goto, H. *Scand. J. Immunol.* **2002**, *56* (4), 327–343.

(19) Wiser, M. F. Plasmodium Life Cycle http://www.tulane.edu/~wiser/malaria/mal_lc.PDF (accessed Sep 6, 2017).

(20) Bartoloni, A.; Zammarchi, L. *Mediterr J Hematol Infect Dis Open J. Syst. Mediterr. J. Hematol. Infect. Dis. Mediterr J Hematol Infect Dis* **2012**, *4* (41),

2035–3006.

(21) Malwest. Plasmodium Life cycle http://www.malwest.gr/en-us/malaria/informationforhealthcareprofessionals/plasmodiumlifecycle.aspx (accessed Sep 22, 2017).

(22) WHO. Diagnostic testing http://www.who.int/malaria/areas/diagnosis/en/ (accessed Sep 22, 2017).

(23) Wanja, E. W.; Kuya, N.; Moranga, C.; Hickman, M.; Johnson, J. D.; Moseti, C.; Anova, L.; Ogutu, B.; Ohrt, C. *Malar. J.* **2016**, *15*, 456466.

(24) Prevention, C.-C. for D. C. *Glob. Heal. - Div. Parasit. Dis. Malar.* **2015**.

(25) Smith Gueye, C.; Newby, G.; Gosling, R. D.; Whittaker, M. A.; Chandramohan, D.; Slutsker, L.; Tanner, M. *Malar. J.* **2016**, *15* (1), 2.

(26) White, M. T.; Verity, R.; Churcher, T. S.; Ghani, A. C. *Vaccine* **2015**, *33*, 7544–7550.

(27) Donnelly, M. J.; Isaacs, A. T.; Weetman, D. *Trends Parasitol.* **2016**, *32* (3), 197–206.

(28) Crompton, P. D.; Moebius, J.; Portugal, S.; Waisberg, M.; Hart, G.; Garver, L. S.; Miller, L. H.; Barillas, C.; Pierce, S. K. *Annu Rev Immunol* **2014**, *32*, 157–187.

(29) Clemente, M.; Corigliano, M. G. *J. Biomed. Biotechnol.* **2012**, *8*.

(30) Greenwood, Brian M.; Bojang, Kalifa Whitty, Christopher J. M.; Targett, G. A. T. *Lancet* **2005**, *365*, 1487–1498.

(31) WHO. Malaria vaccine development http://www.who.int/malaria/areas/vaccine/en/ (accessed Sep 22, 2017).

(32) Pieroni, M.; Azzali, E.; Basilico, N.; Parapini, S.; Zolkiewski, M.; Beato, C.; Annunziato, G.; Bruno, A.; Vacondio, F.; Costantino, G. *J. Med. Chem.* **2017**, *60*, 1959–1970.

(33) Anju Singh, Mudasir Maqbool, Mohammad Mobashir, N. H. *Eur. J. Med. Chem.* **2016**, *125*, 640–651.

(34) Njoroge, M.; Njuguna, N. M.; Mutai, P.; Ongarora, D. S. B.; Smith, P. W.; Chibale, K. *Chem. Rev.* **2014**, *114*, 11138–11163.

(35) Okombo, J.; Chibale, K. *Am. Chem. Soc.* **2017**, *50*, 1606–1616.

(36) Mitali Mishra; Vikash K. Mishra; Varsha Kashaw; Arun K. Iyer; Sushil Kumar Kashaw. *Eur. J. Med. Chem.* **2016**, *125*, 1300–1320.

(37) Dondorp, A. M.; Yeung, S.; White, L.; Nguon, C.; Day, N. P. J.; Socheat, D.; von Seidlein, L. *Nat. Rev. Microbiol.* **2010**, *8* (4), 272–280.

(38) Sidhu, A. B. S.; Verdier-Pinard, D.; Fidock, D. A. *Science* **2002**, *298* (5591), 210–213.

(39) White, N. *R. Soc.* **1999**, *354*, 739–749.

(40) Marco A. Biamonte a, ⇑; Jutta Wanner b; Karine G. Le Roch. *Bioorganic Med. Chemistry Lett.* **2013**, 2829 - 2843.

(41) Njoroge, M.; Njuguna, N. M.; Mutai, P.; Ongarora, D. S. B.; Smith, P. W.; Chibale, K. *Chem. Rev.* **2014**, *114* (22), 11138–11163.

(42) Svogie, A. L.; Isaacs, M.; Hoppe, H. C.; Khanye, S. D.; Veale, C. G. L. *Eur. J. Med. Chem.* **2016**, *114*, 79–88.

(43) Szymański, P.; Markowicz, M.; Mikiciuk-Olasik, E. *Int. J. Mol. Sci.* **2012**, *13* (1), 427–452.

(44) Mayr, L. M.; Bojanic, D. *Curr. Opin. Pharmacol.* **2009**, *9* (5), 580–588.

(45) Liu, B.; Li, S.; Hu, J. *Am. J. Pharmacogenomics* **2004**, *4* (4), 263–276.

(46) TDI. High Throughput Screening - Target Discovery Institute https://www.tdi.ox.ac.uk/high-throughput-screening-2 (accessed Oct 7, 2017).

(47) Carnero, A. *Clin. Transl. Oncol.* **2006**, *8* (7), 482–490.

(48) Mancama, D. D. Towards malaria eradication: Exploiting advances in disease modelling to develop a new generation of drugs against malaria transmission http://conference.csir.co.za/speakers/dr-dalu-mancama/ (accessed Oct 9, 2017).

(49) Che, P.; Cui, L.; Kutsch, O.; Cui, L.; Li, Q. *Assay Drug Dev. Technol.* **2012**, *10* (1), 61–68.

(50) Pérez-Moreno, G.; Cantizani, J.; Sánchez-Carrasco, P.; Ruiz-Pérez, L. M.; Martín, J.; El Aouad, N.; Pérez-Victoria, I.; Tormo, J. R.; González-Menendez, V.; González, I.; De Pedro, N.; Reyes, F.; Genilloud, O.; Vicente, F.; González-Pacanowska, D. *PLoS One* **2016**, *11* (1), e0145812.

(51) Kotz, J. *Sci. Exch.* **2012**, *5* (15), e101038.

(52) Swinney, D. C. *Clin. Pharmacol. Ther.* **2013**, *93* (4), 299–301.

(53) Lee, J. A.; Uhlik, M. T.; Moxham, C. M.; Tomandl, D.; Sall, D. J. *J. Med. Chem.* **2012**, *55*, 4527–4538.

(54) Maryanoff, B. E. *Med. Chem. Lett.* **2016**, *7*, 662–665.

(55) Guiguemde, W. A.; Shelat, A. A.; Garcia-Bustos, J. F.; Diagana, T. T.; Gamo, F.-J.; Guy, R. K. *Chem. Biol.* **2012**, *19* (1), 116–129.

(56) University of Washington. Department of Medicinal Chemistry https://sop.washington.edu/department-of-medicinal-chemistry/ (accessed Oct 14, 2017).

(57) Pussard, E.; Verdier, F. *Fundam. Clin. Pharmacol.* **1994**, *8*, 1–17.

(58) Lynch, D. *Trinity Student Sci. Rev.* **2016**, *2*, 196–210.

(59) Kurth, F.; Pongratz, P.; Bélard, S.; Mordmüller, B.; Kremsner, P. G.; Ramharter, M. *Malar. J.* **2009**, *8*, 10.1186/1475-2875-8-79.

(60) Croft, S. L.; Duparc, S.; Arbe-Barnes, S. J.; Craft, J. C.; Shin, C.-S.; Fleckenstein, L.; Borghini-Fuhrer, I.; Rim, H.-J. *Malar. J.* **2012**, *11*, 10.1186/1475-2875-11-270.

(61) Ayyoub, A.; Methaneethorn, J.; Ramharter, M.; Djimde, A. A.; Tekete, M.; Duparc, S.; Borghini-Fuhrer, I.; Shin, J.-S.; Fleckenstein, L. *Antimicrob. Agents Chemother.* **2016**, *60*, 1450–1458.

(62) Pai, N. R.; Sawant, S. S. *Pharma Chem.* **2014**, *6*, 176–187.

(63) Fidock, D. A.; Nomura, T.; Wellems, T. E. *Mol. Pharmacol.* **1998**, *54*, 1140–1147.

(64) MMV. History of antimalarials https://www.mmv.org/malaria-medicines/history-antimalarials (accessed Oct 27, 2017).

(65) Chulay, J. D.; Watkins, W. M.; Sixsmith, D. G. *Am. J. Trop. Med. Hyg.* **1984**, *33*, 325–330.

(66) Brown, G. D. Artemisinin and a new generation of antimalarial drugs https://eic.rsc.org/feature/artemisinin-and-a-new-generation-of-antimalarial-drugs/2020095.article (accessed Oct 27, 2017).

(67) Vlok, M. C. *Literature Review: Artemisinin*; http://dspace.nwu.ac.za/bitstream/handle/10394/9543/Vlok_MC_3_Literature_Review.pdf?sequence=3 (accessed Oct 27 2017).

(68) Vennerstrom, J. L.; Arbe-Barnes, S.; Brun, R.; Charman, S. A.; Chiu, F. C. K.; Chollet, J.; Dong, Y.; Dorn, A.; Hunziker, D.; Matile, H.; McIntosh, K.; Padmanilayam, M.; Santo Tomas, J.; Scheurer, C.; Scorneaux, B.; Tang, Y.; Urwyler, H.; Wittlin, S.; Charman, W. N. *Nature* **2004**, *430*, 900–904.

(69) Charman, S. A.; Arbe-Barnes, S.; Bathurst, I. C.; Brun, R.; Campbell, M.; Charman, W. N.; Chiu, F. C. K.; Chollet, J.; Craft, J. C.; Creek, D. J.; Dong, Y.; Matile, H.; Maurer, M.; Morizzi, J.; Nguyen, T.; Papastogiannidis, P.; Scheurer, C.; Shackleford, D. M.; Sriraghavan, K.; Stingelin, L.; Tang, Y.; Urwyler, H.; Wang, X.; White, K. L.; Wittlin, S.; Zhou, L.; Vennerstrom, J. L. *Proc. Natl. Acad. Sci.* **2011**, *108*, 4400–4405.

(70) Baumgärtner, F.; Jourdan, J.; Scheurer, C.; Blasco, B.; Campo, B.; Mäser, P.; Wittlin, S. *Malar J* **2017**, *16*, 10.1186/s12936-017-1696-0.

(71) Kuhen, K. L.; Chatterjee, A. K.; Rottmann, M.; Gagaring, K.; Borboa, R.; Buenviaje, J.; Chen, Z.; Francek, C.; Wu, T.; Nagle, A.; Barnes, S. W.; Plouffe, D.; Lee, M. C. S.; Fidock, D. A.; Graumans, W.; Van De Vegte-Bolmer, M.; Van Gemert, G. J.; Wirjanata, G.; Sebayang, B.; Marfurt, J.; Russell, B.; Suwanarusk, R.; Price, R. N.; Nosten, F.; Tungtaeng, A.; Gettayacamin, M.; Sattabongkot, J.; Taylor, J.; Walker, J. R.; Tully, D.; Patra, K. P.; Flannery, E. L.; Vinetz, J. M.; Renia, L.; Sauerwein, R. W.; Winzeler, E. A.; Glynne, R. J.; Diagana, T. T. *Antimicrob. Agents Chemother.* **2014**, *58*, 5060–5067.

(72) MMV. KAF156 plus lumefantrine. https://www.mmv.org/related-story-type/kaf156 (accessed Nov 6, 2017).

(73) White, N. J.; Duong, T. T.; Uthaisin, C.; Nosten, F.; Phyo, A. P.; Hanboonkunupakarn, B.; Pukrittayakamee, S.; Jittamala, P.; Chuthasmit, K.; Cheung, M. S.; Feng, Y.; Li, R.; Magnusson, B.; Sultan, M.; Wieser, D.; Xun, X.; Zhao, R.; Diagana, T. T.; Pertel, P.; Leong, F. J. *N. Engl. J. Med.* **2016**, *375*, 1152–1160.

(74) Baker, S. J.; Ding, C. Z.; Akama, T.; Zhang, Y.-K.; Hernandez, V.; Xia, Y. *Future Med. Chem.* **2009**, *1*, 1275–1288.

(75) Sonoiki, E.; Ng, C. L.; Lee, M. C. S.; Guo, D.; Zhang, Y.-K.; Zhou, Y.; Alley, M. R. K.; Ahyong, V.; Sanz, L. M.; Lafuente-Monasterio, M. J.; Dong, C.; Schupp, P. G.; Gut, J.; Legac, J.; Cooper, R. A.; Gamo, F.-J.; DeRisi, J.; Freund, Y. R.; Fidock, D. A.; Rosenthal, P. J. *Nat. Commun.* **2017**, *8*, 14574.

(76) Hu, Q.-H.; Liu, R.-J.; Fang, Z.-P.; Zhang, J.; Ding, Y.-Y.; Tan, M.; Wang, M.; Pan, W.; Zhou, H.-C.; Wang, E.-D. *Sci. Rep.* **2013**, *3*, 2475.

(77) Xia, Y.; Cao, K.; Zhou, Y.; Alley, M. R. K.; Rock, F.; Mohan, M.; Meewan, M.; Baker, S. J.; Lux, S.; Ding, C. Z.; Jia, G.; Kully, M.; Plattner, J. J. *Bioorg. Med. Chem. Lett.* **2011**, *21*, 2533–2536.

(78) Gupta, A. K.; Studholme, C. *Expert Opin. Investig. Drugs* **2016**, *25*, 297–305.

(79) Zhang, Y.-K.; Plattner, J. J.; Akama, T.; Baker, S. J.; Hernandez, V. S.; Sanders, V.; Freund, Y.; Kimura, R.; Bu, W.; Hold, K. M.; Lu, X.-S. *Bioorg. Med. Chem. Lett.* **2010**, *20*, 2270–2274.

(80) Paton, D. M. *Drugs of Today* **2017**, *53*, 239–245.

(81) Towler, D. A.; Adamst, S. P.; Eubankst, S. R.; Toweryt, D. S.; Jackson-Machelski, E.; Glasert, L.; Gordon, J. I. *Biochemistry* **1987**, *84*, 2708–2712.

(82) Herrera, L. J.; Brand, S.; Santos, A.; Nohara, L. L.; Harrison, J.; Norcross, N. R.; Thompson, S.; Smith, V.; Lema, C.; Varela-Ramirez, A.; Gilbert, I. H.; Almeida, I. C.; Maldonado, R. A. *PLoS Negl. Trop. Dis.* **2016**, *10*, 1-20.

(83) Wright, M. H.; Clough, B.; Rackham, M. D.; Rangachari, K.; Brannigan, J. A.; Grainger, M.; Moss, D. K.; Bottrill, A. R.; Heal, W. P.; Broncel, M.; Serwa, R. A.; Brady, D.; Mann, D. J.; Leatherbarrow, R. J.; Tewari, R.; Wilkinson, A. J.; Holder, A. A.; Tate, E. W. *Nat. Chem.* **2013**, *6*, 112–121.

(84) Tate, E. W.; Bell, A. S.; Rackham, M. D.; Wright, M. H. *Parasitology* **2014**, *141*, 37–49.

(85) Sharma, V.; Kumar, P.; Pathak, D. *J. Heterolytic Chem.* **2010**, *47*, 491–502.

(86) Kaushik, N.; Kaushik, N.; Attri, P.; Kumar, N.; Kim, C.; Verma, A.; Choi, E. *Molecules* **2013**, *18*, 6620–6662.

(87) Biswal, S.; Sahoo, U.; Sethy, S.; Kumar, H. K. S.; Banerjee, A. M. *Asian J. Pharm. Clin. Res.* **2012**, *5*, 1–6.

(88) Blough, B. E.; Landavazo, A.; Decker, A. M.; Partilla, J. S.; Baumann, M. H.; Rothman, R. B. *Psychopharmacology (Berl).* **2014**, *231*, 4135–4144.

(89) Suzen, S.; Tekiner-Gulbas, B.; Shirinzadeh, H.; Uslu, D.; Gurer-Orhan, H.; Gumustas, M.; Ozkan, S. A. *J. Enzyme Inhib. Med. Chem.* **2013**, *28*, 1143–1155.

(90) Veale, Clinton G.L.; Edkins, Adrienne L.; de la Mare, Jo-Anne; de Kock, Carmen; Smith, Peter J.; Khanye, S. D. *Tetrahedron Lett.* **2015**, *56*, 1860–1864.

(91) Ottoni, O.; De, A.; Neder, V. F.; Dias, A. K. B.; Cruz, R. P. A.; Aquino, L. B. *Org. Lett.* **2001**, *3* (7), 1005–1007.

(92) Veale, C. G. L.; Lobb, K. A.; Zoraghi, R.; Morrison, J. P.; Reiner, N. E.; Andersen, R. J.; Davies-Coleman, M. T. *Tetrahedron* **2014**, *70*, 7845–7853.

(93) Veale, C. G. L.; Zoraghi, R.; Young, R. M.; Morrison, J. P.; Pretheeban, M.; Lobb, K. A.; Reiner, N. E.; Andersen, R. J.; Davies-Coleman, M. T. *J. Nat. Prod.* **2015**, *78*, 355–362.

(94) King, C. L. . O.; Kenneth G. *J. Med. Chem.* **1964**, *48*, 3459–3461.

(95) He, M.; Yang, N.; Sun, C.; Yao, X.; Yang, M. *Med. Chem. Res.* **2011**, *20*, 200–209.

(96) Navre, M. https://www.collaborativedrug.com/buzz/2014/07/14/why-using-pic50-instead-of-ic50-will-change-your-life/.

(97) Fleming, F. F.; Yao, L.; Ravikumar, P. C.; Funk, L.; Shook, B. C. *J. Med. Chem.* **2010**, *53*, 7902–7917.

(98) Daina, A.; Zoete, V. *ChemMedChem* **2016**, *11*, 1117–1121.

(99) Gottlieb, H. E.; Kotlyar, V.; Nudelman, A. *J. Org. Chem.* **1997**, *62*, 7512–7515.

(100) Armarego, W.L.F.; Perrin, D. D. *Purification of Laboratory Chemicals*, 4th ed.; Butterworth-Heinemann, Ed.; British Library Cataloguing in Publication Data Library of Congress Cataloguing in Publication Data: Oxford, 2000.

(101) Casey, M.; Leonard, J.; Lygo, B.; Procter, G. *Advanced Practical Organic Chemistry*; Springer US: Boston, MA, 1990.